Graphene: A Platform for Surface-Enhanced Raman Spectroscopy
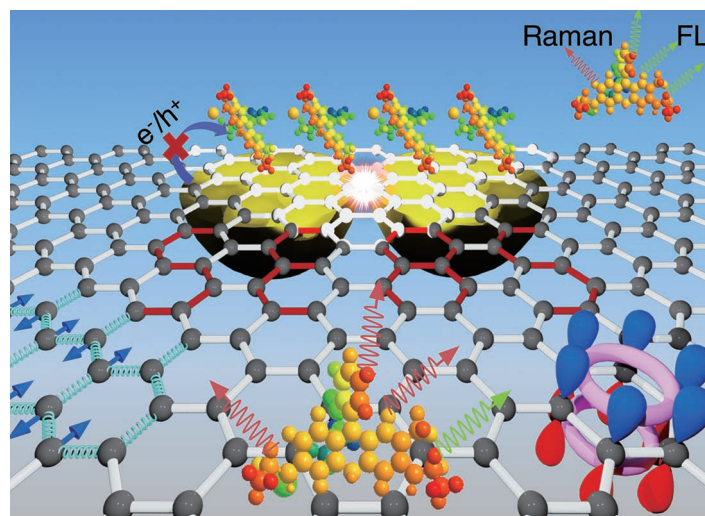
Weigao Xu, Nannan Mao, and Jin Zhang*

From the Contents

Surface-enhanced Raman spectroscopy (SERS) imparts Raman spectroscopy with the capability of detecting analytes at the single-molecule level, but the costs are also manifold, such as a loss of signal reproducibility. Despite remarkable steps having been taken, presently SERS still seems too young to shoulder analytical missions in various practical situations. By the virtue of its unique molecular structure and physical/chemical properties, the rise of graphene opens up a unique platform for SERS studies. In this review, the multi-role of graphene played in SERS is overviewed, including as a Raman probe, as a substrate, as an additive, and as a building block for a flat surface for SERS. Apart from versatile improvements of SERS performance towards applications, graphene-involved SERS studies are also expected to shed light on the fundamental mechanism of the SERS effect.

1. Introduction

Raman spectroscopy is exploited for rapid, precise and robust molecular identification, yet the bottleneck is the quite small cross-section of common molecules and sequentially rather weak Raman signal. Surface-enhanced Raman spectroscopy (SERS)[1,2] can hugely boost the Raman fingerprints of molecules, which offers ultrasensitive detection (even down to the single-molecule level[3,4]) with molecular selectivity. The first SERS experiment could be said to date back to 1974,[5] done by Fleischmann et al., about three years before the proposition of the concept of the SERS effect.[1,2] In their experiment, an electrochemically roughened silver electrode and pyridine were used as the enhancement media (usually called a SERS substrate) and the probe molecule, respectively, to produce a dramatically enhanced Raman signal. During the past nearly four decades, great efforts and ingenuity have gone towards both understanding the origin of the SERS effect and creating a more desirable SERS substrate, resulting in continuing theoretical and experimental progress. Yet SERS has not entered the widespread real-world application stage. The main reason lies in the difficulty in achieving a quantitative understanding of the controversial mechanism of SERS and the difficulty to develop a perfect SERS method which can simultaneously meet the following requirements:[6,7] 1) high SERS activity to ensure an acceptable sensitivity; 2) uniformity to provide reproducible signals; 3) high selectivity with a clear 'molecular structure'–'SERS features' relationship; 4) preferable measurement procedure with quick/friendly sample pretreatments and compatibility under various conditions. The emergence of a large class of new SERS probes and new SERS substrates brings about both a more insightful understanding of the fundamental mechanism and an optimized model/procedure for applications of SERS. Ultrasensitive substrates competent for a single-molecule level response are routinely studied[8] and matured preparation skills of large-scale metal nanostructure arrays towards better signal uniformity have been developed.[7] Numerous pioneering attempts to study the structure–function relationship of plasmonic metals[9] and electronic state-related chemical mechanisms[10] have been implemented. As a new point of view, strategies towards metal molecule isolation (for more intrinsic SERS signals)[11] have been demonstrated recently. Furthermore, flexible substrates have proven to be a fascinating choice for the exploration of SERS in real-world applications.[12] All of which is impactful progress, yet there remains great limitations to the full exploration of SERS.

In most situations, a new characterization technique brings about a revolution in materials science; on the contrary, a new material can upgrade the performance of new technologies. This synergistic action is also prominent in the research between graphene and SERS. Graphene, as another kind of carbon allotrope discovered experimentally in 2004,[13] is a perfect 2D atomic crystal made of sp^2 carbon atoms. Besides the abundant theoretical and experimental interests in its electronic properties,[14] it is also a rising star in SERS. The roles of graphene in SERS are manifold. The following distinctive structural features and properties of graphene provide it with some unique advantages for SERS: 1) its unique electron and phonon structures; 2) atomic uniformity; 3) biological compatibility; 4) delocalized π bonds; 5) its seamless structure; 6) atomic thickness; 7) chemical inertness. Actually, most of the above aspects have been partially proven and the rest are being explored. As a new figure in SERS, graphene is opening up a unique platform for it. In this review, we will summarize the progress on graphene-involved SERS studies in the following sequence as classified by the role of graphene, as: 1) a Raman probe; 2) a substrate; 3) an additive; 4) a building block for SERS on a flat surface.

2. Graphene as a Raman Probe

Graphene, a single sheet of carbon atoms in a 2D honeycomb crystal structure, has exhibited amazing Raman scattering properties, which are related to its unique structure of electrons and phonons. In this part, we will review recent progress on this topic in two sections: the Raman scattering features of graphene, and the SERS studies with graphene as a probe molecule.

2.1. Raman Scattering Features of Graphene

2.1.1. Typical Raman Spectrum of Graphene

Figure 1 shows a typical Raman spectrum of defect-containing graphene measured with a 514.5 nm laser. Two characteristic peaks named the G band (~1585 cm^{-1}) and the G′ band (~2685 cm^{-1}) are intrinsic vibrations of defect-free graphene. If the Raman spectrum is achieved in disordered graphene or at the edges, we may find that several other peaks appear at ~1345 cm^{-1} (D band) and ~1625 cm^{-1} (D′ band), respectively. The emergence of 1450 cm^{-1} (D$_2$ band) and 1500 cm^{-1} (D$_3$ band) has also been reported.[15] Among these bands, the G band originates from a first-order Raman scattering process, corresponding to the degenerate iTO and iLO phonons at the Γ point (degenerate E$_{2g}$ mode).[16,17] The G′ band is due to a double resonance intervalley Raman scattering process with two iTO phonons at the K point.[18] As illustrated in the insets in Figure 1, the D band, D′ band, and G′ band are all second-order processes.[19–21] It is notable that, despite the G′ band being sometimes referred to as the "2D band", it is not the second-order mode of the D band.

W. G. Xu, N. N. Mao, Prof. J. Zhang
Center for Nanochemistry
Beijing National Laboratory for Molecular Sciences
Key Laboratory for the Physics
and Chemistry of Nanodevices
State Key Laboratory for Structural Chemistry
of Unstable and Stable Species
College of Chemistry and Molecular Engineering
Peking University
Beijing 100871, China
E-mail: jinzhang@pku.edu.cn

The G′ band appears in a perfect graphene sample while the D band is absent, since the G′ band has nothing to do with defects of graphene.[20] Another first-order band is the low frequency E_{2g} mode (located at ~42 cm^{-1}), involving the weak interlayer interaction, so usually it cannot be observed on a Raman spectrum of graphene.[22] Another small peak at ~3250 cm^{-1} is the second-order mode of the D′ band.[23]

2.1.2. Probing the Number of Layers, Edges and Defects, and Doping Effects

Raman spectroscopy is a convenient tool to probe the structure of graphene, which has a significant effect on its properties. As a Raman probe, the Raman features of graphene itself are interesting and informative. On the basis of these Raman fingerprints, we can distinguish the number of graphene layers, probe the type of edges (and defects) and monitor the degree of doping quickly and directly.

For graphene with a different number of layers (n), the G′ band shows a different shape, position and intensity, according to which Ferrari et al.[24] suggested that we can find out the accurate number of layers in few layer graphene samples. As **Figure 2**a shows, for monolayer graphene, the G′ peak is a perfect single Lorentzian feature, while the G′ peak of bilayer graphene shows a broad band containing four components.[24,25] To be appealing, the G′ band of three-layer graphene needs more Lorentzians to fit.[20] When n comes to five or more, the G′ band shows the same features as graphite; it is no longer easy to distinguish it from graphite. This phenomenon can be explained by a double resonance mechanism under the condition that the electronic structure of graphene sheets would vary with n.[20,23,24] At the same time, when n grows, the G band frequency downshifts[15] and its intensity is almost linear as n ranges from 1–10.[26] Koh et al.[27] demonstrated how to identify the value of n via the Raman intensity ratio of graphene G band and Si substrate, i.e., I(G)/I(Si). Besides, the weak disorder-induced D_3 peak also shows unexpected sensitivity to n, and the total intensity of the series of D bands decrease as n increases.[15] Gupta et al.[22] discovered that the shape of D band also varies for different graphene thicknesses. Recently, the shear mode at the low frequency region[28] and layer breathing mode at 1720 cm^{-1}[29] are also effective ways to identify the thickness of graphene layers.

Weigao Xu received his BS from Lanzhou University in 2008. Since then, he joined Prof. Jin Zhang's group for a 5-year PhD program in the College of Chemistry and Molecular Engineering, Peking University. His current research is focused on the design, fabrication, and applications of graphene-involved SERS substrates, including SERS on a flat surface, the substrate-dependence of SERS performance, and plasmon-assistant chemical processes in SERS.
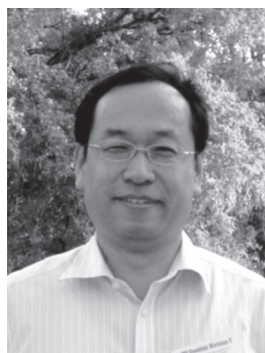
Jin Zhang received his PhD from Lanzhou University in 1997. After a two year postdoctoral fellowship at the University of Leeds, UK, he joined to Peking University where he was appointed Associate Professor (2000) and promoted to Full Professor in 2006. His research focuses on the controlled synthesis and spectroscopic characterization of carbon nano-materials. Dr. Zhang has received the National Science Foundation of China for Distinguished Young Scholars in 2007 and 2nd grade of the State Natural Science Award in 2008 (2nd contributor). Dr. Zhang has published over 140 peer-reviewed journal articles. And he now is editor of Carbon.

The D band appears in the Raman spectrum of a graphene edge, or a graphene piece that contains defects. Cançado et al.[30] found that different graphite edges show distinguishable D bands. As we all know, the D band is due to a second-order scattering process which involves a defect and a phonon. The wave vectors of the armchair and zigzag defect edges are different: the former connects K point and K′ point, while the latter does not and thus cannot meet the law of conservation of momentum. Thus the D band is dependent on the structure of the graphene edge, e.g., armchair edges show a clear D band while zigzag edges do not. You et al.[31] discovered that it is possible to use Raman spectroscopy to determine the orientation of graphene (either
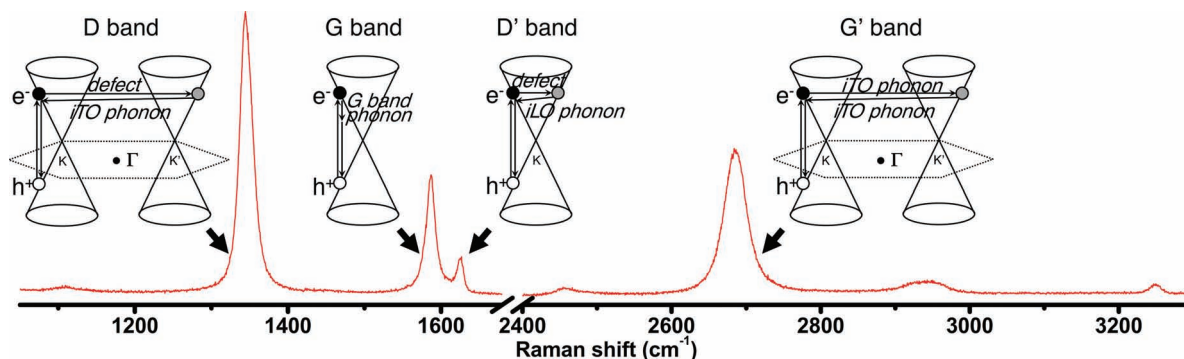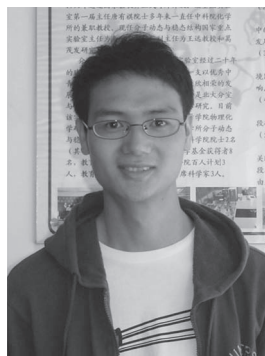

Figure 1. Typical Raman spectrum of defect-containing graphene measured with a 514.5 nm laser. CVD-grown graphene sample for Raman measurement was transferred on a SiO$_2$(300 nm)/Si substrate, and then treated with O$_2$ plasma. Illustrations of the first-order Raman scattering process of G band and second-order Raman scattering processes of D, D', G' band in graphene are shown together, adapted with permission.[20] Copyright 2009, Elsevier.
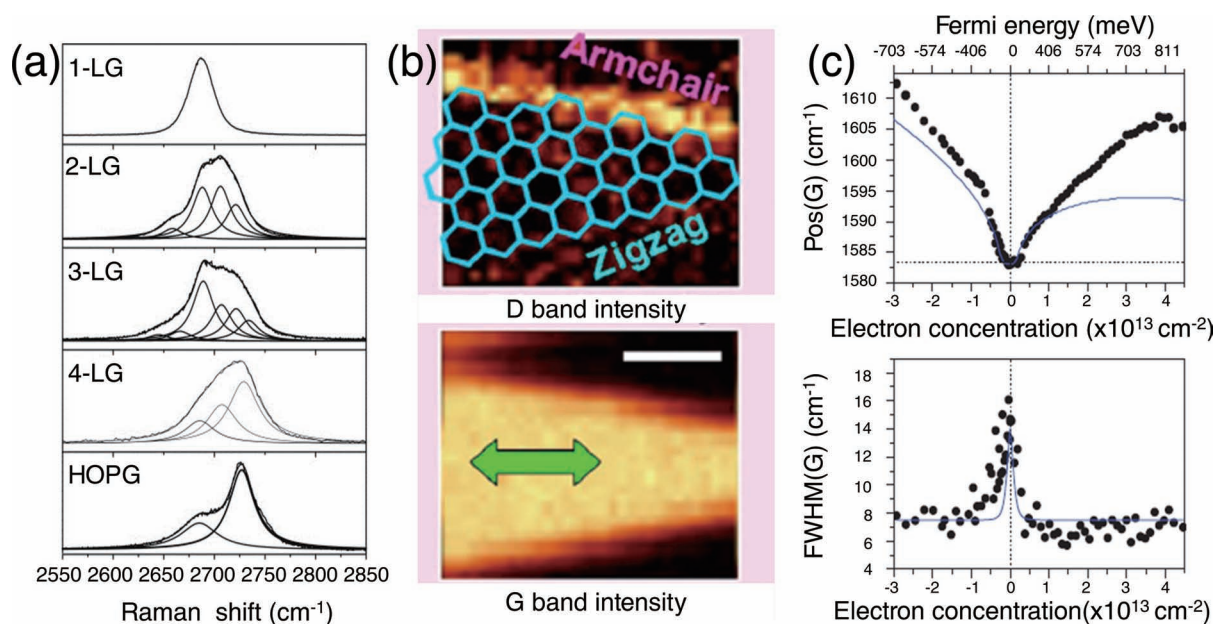
Figure 2. a) Layer-dependent G′ band of 1, 2, 3, 4-layer graphene and HOPG, under 514.5 nm excitation. Reproduced with permission.[20] Copyright 2009, Elsevier Ltd. b) Raman mapping of graphene edges with an angle of 30°. The scale bar is 1 μm. Reproduced with permission.[31] Copyright 2008, American Institute of Physics. c) The position and FWHM (full width at half maximum) of G band of intrinsic graphene as a function of doing concentration induced by electrochemical top gate voltage. Reproduced with permission.[42] Copyright 2008, Nature Publishing Group.

zigzag or armchair predominant edges; Figure 2b). In addition, the intensity of the D band is related to the polarization of the incident and scattered light.[32] Krauss et al.[33] successfully achieved zigzag predominant edges by anisotropic etching and proved that zigzag edges do not contribute to the D band, which further confirms the correctness of the theory on the D band Raman process. It was also reported that the two edges which have been thought as an armchair and a zigzag edges do not show dramatic difference in D band.[32] However, we think the problem does not lie in the D band theory, but whether the analyzed edge is predominantly one or the other type of graphene edge. Besides graphene edges, artificial defects in graphene will also result in the emergence of D and D′ bands.[34]

The level of doping also has an important influence on the properties of graphene. Graphene made by different methods or under different environments possesses different amount of doping.[35,36] Even different points of the same piece of graphene show dramatically different degrees of doping, induced by the substrate and adsorbates,[37,38] let alone different pieces of graphene.[39] Monitoring the level of doping is very important, and Raman spectroscopy has been proved to be capable of this, which in turn helps us to investigate electron–phonon interactions in graphene.[40–42] It should be noted that, despite that in most cases natural chemical doping effects (either from substrate or adsorbates) are important, here we just discuss examples on electric-gate-induced doping samples (since electric gates can induce doping in a controllable way, while they have a similar physical origin). Yan et al.[40] discovered that the G and G′ band shifts of graphene show obvious dependence on the induced charge density modulated by the electric field effect. The G band upshifts and its full width at half maximum decreases,

no matter whether the graphene is p-type or n-type doped. As shown in Figure 2c, Das et al.[42] also demonstrated the same phenomenon in an electrochemically top-gated graphene transistor. At the same time, the G′ band can be used to assign p- or n-type doping, which upshifts for p-doping and downshifts for n-doping. The intesity ratio $I_{G'}/I_G$ can be use to obtain the doping concentration.[42] Ferrari et al.[39,43] thought that the phenomenon could be better understood by quantum mechanics beyond the adiabatic Born–Oppenheimer approximation.

In short, Raman spectroscopy is a sensitive tool to probe the number of graphene layers, edges, disorder, and doping. The diversity of behaviors of electrons and phonons in graphene offers an intriguing stage for learning the basic Raman scattering effects. Furthermore, mature techniques towards the controlled synthesis and functionalization of graphene are developing, which opens up a great opportunity to exploit the Raman characteristics of graphene in a well-designed way.

2.2. Graphene as a Probe in SERS

Besides pyridine, various SERS probes have been explored. The standards to guarantee a good SERS probe are usually case dependent. When the Raman behavior of the probe itself, or when the qualitative/quantitative information of the components of a sample are considered, the probe is a fixed parameter. For cases when we are investigating the fundamental details of the SERS effect, mostly a carefully selected probe benefits a lot, according to the particular problem we are studying. Otherwise, if we are using a SERS probe as a target for a certain process, the pristine cross-section and

its compatibility with the target environment are essential considerations, for instance, dyes are normally preferred for such cases (e.g., bioimaging). In this part, we will review the recent progress in the SERS study with graphene as a probe, including both the investigation of the intriguing Raman features of graphene itself and SERS-related issues probed by graphene.

2.2.1. Probing the Fine Structure of Graphene

The performance of graphene for most applications (especially nanoelectronics) is highly structure-sensitive and, as discussed in the earlier section, we have found that these fine structures of graphene can be well revealed in its Raman spectrum. The pursuit of a stronger Raman signal of graphene itself is thus a subject with broad interest.

The first consideration that affects the Raman intensity of graphene is an appropriate substrate. Looking back on many published works on graphene, most of them used a silicon substrate with a 300 nm oxide layer. The oxide layer is essential for both the optical visibility of single layer graphene[44–47] and an enhancement of the Raman intensity through a thin-film interference effect.[26,48] Defining n_{SiO2} as the refractive index of silicon dioxide and d as its thickness, a maximum of interference enhancement (reaching a factor of 30[26]) occurs when $n_{SiO_2} \bullet d = (2n+1)\lambda/4$, $n = 0, 1, 2, 3$, where λ is the wavelength of the excitation laser. For example, a 269 nm oxide layer is one of the most desirable thicknesses for 532 nm excitation.[26] Actually, in many experimental studies on the Raman enhancement of graphene, the accompanied interference enhancement should be taken into consideration, yet this effect has been sometimes inappropriately neglected.

Such an enhancement level is not satisfying. The surface plasmon resonance enhancement was then introduced by Cheng's group in a so-called "SERS and interference co-enhanced Raman scattering, SICERS" experiment.[49,50] By the construction of a Si/Ag/Al$_2$O$_3$/graphene structure, a total enhancement factor on the order of 10^3 (compared with Si substrate) can be obtained. However, this kind of sample configuration does not employ the localized surface plasmon resonance effect. Localized electromagnetic field enhancement achieved by an SPM tip (tip-enhanced Raman spectroscopy, TERS) was demonstrated by Domke et al.[51] (an enhancement factor of 6×10^3 was reported for the tip region) and Saito et al.[52] Thermally evaporated gold films were also deposited on single layer graphene and a maximum enhancement of 120 times was reported by Lee et al.[53] They also reported that the interference enhancement contribution is ~1.6 among a total averaged enhancement factor of 71. Yet this is not a rigorous comparison since different substrates were used (glass vs. silica) and the shelter effect for the incident laser from the gold nanoislands was ignored. Thereafter, abundant SERS studies for the detailed investigation of graphene have been implemented.[54–62]

With a much stronger Raman signal, SERS is expected to visualize the fine structure of graphene. In Ren et al.'s experiments,[49] the SICERS method was exploited to study the edge phonon state of graphene nanoribbons; according to their experimental observations and first-principles calculations the emerging bands at 1450 and 1530 cm^{-1} were assigned to vibrations from edge atoms. Lee et al.[53] observed the emergence of a D band after the deposition of a SERS-active gold film on graphene, and it was claimed that this was due to a SERS enhancement effect, rather than possible mechanical damages induced by the thermal evaporation of gold. Similarly, a selective enhancement of the D band was reported by Ouyang et al.:[56] the I$_D$/I$_G$ ratio increased from 0.76 to 2.18 for few layer graphene samples (prepared by deoxidizing graphite oxide) on silver. New emerging bands at lower frequencies (239 cm^{-1} and 992 cm^{-1}) were also observed. Layer-dependent SERS intensity[53,63] showed that monolayer graphene has a stronger enhancement factor than multilayer graphenes. On the other hand, TERS studies offer us insightful structural understandings of graphene with subdiffraction resolution.[52,57] For example, in Satio et al.'s experiments,[51] a spatial resolution of around 30 nm can be achieved. The layer boundary-dependent G-band intensity, the charge effect-dependent G-band position and width, as well as the local stress distribution-dependent G'-band fluctuations were investigated in detail. Interestingly, Wang et al.[60] studied the reversible creation and disappearance of a single defect based on the manipulation of contact/retract states of a TERS tip. In this case, the TERS tip is both a defect inducer and a signal magnifier.

These achievements are important steps towards a better understanding of the fine structure of graphene. Nevertheless, there remains more to be explored, such as the discovery and assignment of veiled features of pristine graphene and new features induced by metal–graphene interactions.

2.2.2. Probing the Relationship between Substrate Structure and SERS Performance

The evaluation of a 'substrate structure'–'SERS performance' relationship is of great interest, not only for the development of a reliable quantitative SERS method, but also for chemical and physical insights into the surface plasmon resonance effect. However, until now rare studies have been done on this point. One of the biggest obstacles is the arrangement of probe molecules and their stability under SERS measurement conditions. The adsorption behavior of molecules on a curved/gapped SERS substrate is complicated, with fluctuating amounts and molecular orientations. Furthermore, for common probes (especially for dyes), laser-induced damage during SERS measurements is often inevitable and may cause trouble in quantitative analyses.

Graphene offers us a new choice: the 2D graphene layer is uniform and chemically inert. The capacity of graphene to probe the SERS activity is also being explored. In Schedin et al.'s[54] experiments (**Figure 3**), gold nanoparticle arrays with different sizes (140 nm and 210 nm) were fabricated to demonstrate the structure-dependent SERS activity. They found that their experimental observations are in good agreement with theoretical simulation results. In our experiments, the SERS signal of graphene was used as a reference to investigate the thickness-dependent SERS activity of thermal vacuum evaporated gold films. By varying the gold film thickness from 0 to 20 nm, we found a preferred thickness of 8 nm.[64] In addition, when putting graphene on the
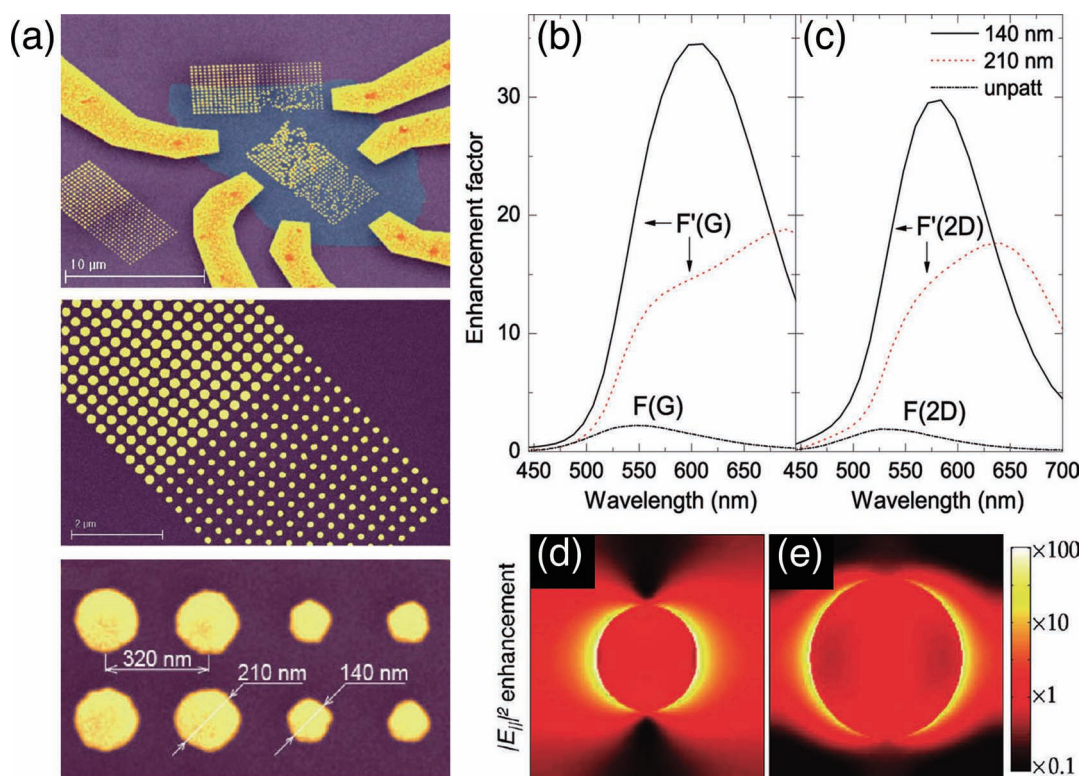
Figure 3. Size-dependent SERS enhancement of gold nanoparticles probed by graphene. a) SEM images (in false colors) of the SERS sample: purple, SiO_2; bluish, graphene; yellow, Au electrodes and dots. Arrays of 210 nm and 140 nm gold nanodisks are tested. b,c) The enhancement factors for (b) the G and (c) 2D(G') peaks. d,e) Field intensity distribution at 633 nm for the (e) 140 nm and (f) 210 nm nanodisks. Reproduced with permission.[54] Copyright 2010, American Chemistry Society.

top of such an evaporated island-like gold film, it is interesting to investigate the position-sensitive SERS activity of the gold film substrate by an in-situ thermal annealing process, in which the flexible graphene layer was gradually moved closer to the hot spot, resulting in an increasing SERS intensity.[65] To exclude the disturbance of chemical enhancement, recently Niu et al.[59] added an Al_2O_3 inserting layer between the gold nanoparticles and SiC epitaxial graphene. The calculated electromagnetic enhancement (based on the dipole approximation) agreed well with the experiments for excitation energy-dependent enhancement. By varying the thickness of the Al_2O_3 layer from 0, 3, 6, 9 to 12 nm, they also found there is an exponential relationship between enhancement factor and distance of graphene/gold nanoparticles.

2.2.3. Probing the Life Process

Another advantage of graphene is its biological compatibility. Actually graphene has been widely used in many biological fields, including drug delivery,[66] biosensing[67] and bioimaging[68] applications. Nevertheless, little has been done towards understanding the detailed process of cell uptake of graphene. The enlargement of pristine weak Raman signals of graphene by SERS is helpful in sensing applications. Other materials like carbon nanotubes were also explored in the related studies. The competition between graphene and others is under way and it is too early to say who will be the winner, or maybe they will find their own stage. In this part, we will bypass the details of why graphene was selected, and

will just focus on an example of how the biological process can be monitored by SERS.

Huang et al.[58] investigated the cell uptake mechanism of graphene oxide (GO) by SERS (**Figure 4**). They found that the loading of gold nanoparticles was essential for the visibility of the Raman signal of GO inside the Ca Ski cell. A time series of incubation for 1, 2, 4, 6, 8 and 12 h showed no detectable SERS signal of GO until after 4 h. The SERS signal reached at a maximum at 6 h; further incubation resulted in a weakened SERS signal, and it was barely on the noise level after 12 h incubation. Interestingly, by the addition of different kinds of inhibitors of distinguished endocytotic mechanisms, they found that the cell uptake process of GO is based on the clathrin-mediated mechanism and is energy dependent. During these experiments, the availability of SERS signals and their intensity were probabilistic (mainly because of an inhomogeneous distribution of Au-GO composites in the cell), and statistical results were exploited for related analyses.

Above is one of the pioneering examples of graphene-involved SERS for biosystem applications. Despite the world-wide interest on biorelated issues, current progress on this topic via graphene-involved SERS methods have hardly been reported. Such unbalanced development (as compared to other graphene-probed issues) may partially because of a much longer experimental period for bio-researches. However, we believe that the importance on this field is indubitable and continued progress is expected to be on the way.
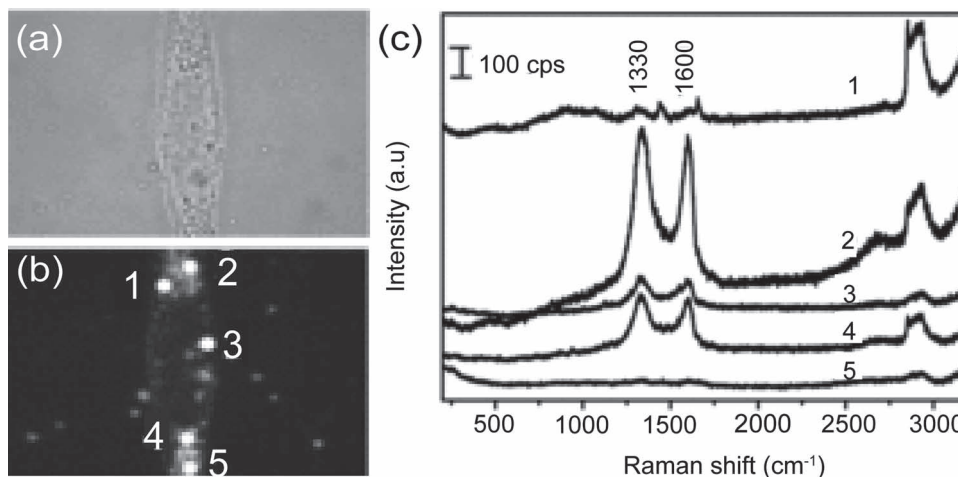
Figure 4. a,b) Bright and dark-field microscopic images of Ca Ski cells incubated with Au-GO for 4 h, respectively. c) SERS spectra of the different points of GO in the Ca Ski cell in (b). Reproduced with permission.[58] Copyright 2012, Wiley-VCH.

On the other hand, the special 2D structure of graphene pieces can be reduce to 0D, e.g., graphene quantum dots and graphene@Au(Ag) core–shell nanoparticles are both desirable subjects for further investigations.

3. Graphene as a Substrate: Graphene-Enhanced Raman Scattering (GERS)

When considering its 2D structure, graphene is a likely substrate. There have been wide achievements on miscellaneous SERS substrates with different materials, morphologies, and preparation methods. For example, a series of materials can be used as a SERS substrate, from noble metals (Ag, Au, Cu) to transition metals (Pt, Pd, Ru, Rh, Fe, Co, Ni, etc), to semiconductors (Si, Ge, ZnO, TiO_2, CuO, CdTe, etc).[69–71] Actually, considerable electromagnetic enhancement exists only for the original noble metal substrates. For the rest of the materials, a chemical-based mechanism is dominant in the total SERS enhancement, with a much lower enhancement factor.

In graphene, the remaining one $2p_z$ orbital of each sp^2 hybridized carbon atom constitutes a large delocalized π bond. Investigations on the interactions between graphene and adsorbed molecules have been carried out and, interestingly, the phenomenon of Raman enhancement on graphene substrates has been observed. In this part we will focus on the second role of graphene played in SERS, i.e., as a substrate. The discovery of GERS effect, its chemical mechanism-based enhancement features, and applications in probing the molecular behaviors are discussed.

3.1. The Discovery of the GERS Effect

3.1.1. The Fluorescence Quenching Effect of Molecules Adsorbed on Graphene

Actually, the spectral behavior of molecules would change when they were put on a graphene surface. Xie et al.[72] first

observed a fluorescence quenching effect of fluorescent dyes (rhodamine 6G, R6G; and protoporphyrin IX, PPP) adsorbed on graphene, and obtained their Raman signals. Since much larger cross-sections of fluorescence signals are observed as compared to Raman signals, the Raman characteristics are often interfered with or even submerged by the intense fluorescence background. How to get the Raman signal of molecules from their fluorescence background has been considered as a long-term question. Previously in such cases, non-resonance excitation is a solution, but will cause a certain loss of sensitivity. Besides, ultraviolet resonance Raman spectroscopy (UV-RRS),[73] time-resolved Raman detection,[74] coherent anti-Stokes Raman spectroscopy (CARS)[75] and femtosecond-stimulated Raman spectroscopy (FSRS)[76] have been developed to avoid the fluorescence disturbances, while these approaches are usually apparatus-dependent or have other limitations.

For fluorescent dyes (such as R6G) adsorbed on graphene, the 2D sheet of sp^2 carbon atoms and the aromatic molecules constitute a system with considerable π–π interactions. From Xie et al.'s results,[72] the fluorescence quenching effect for minimum R6G adsorbed on graphene was found to be impressive, and a roughly estimated quenching factor on the order of 10^3 was reported: detailed processes are illustrated in **Figure 5**. This is basically due to a resonance energy transfer process, as in accordance with theoretical observations from Swathi et al.,[77] in which a fast resonance energy transfer process from dyes to graphene was reported. Thus, a graphene substrate provides a direct and effective way to measure the Raman scattering spectra of fluorescent dyes under resonant excitation, which are normally difficult to acquire.

3.1.2. The GERS Effect

Graphene–molecule interactions are also an origin for graphene-enhanced Raman scattering (GERS; **Figure 6**). The discovery of GERS effect by Ling et al.[78] began with an accidental experiment, in which it was found that, there were many 'emerging bands' of mechanically exfoliated graphene
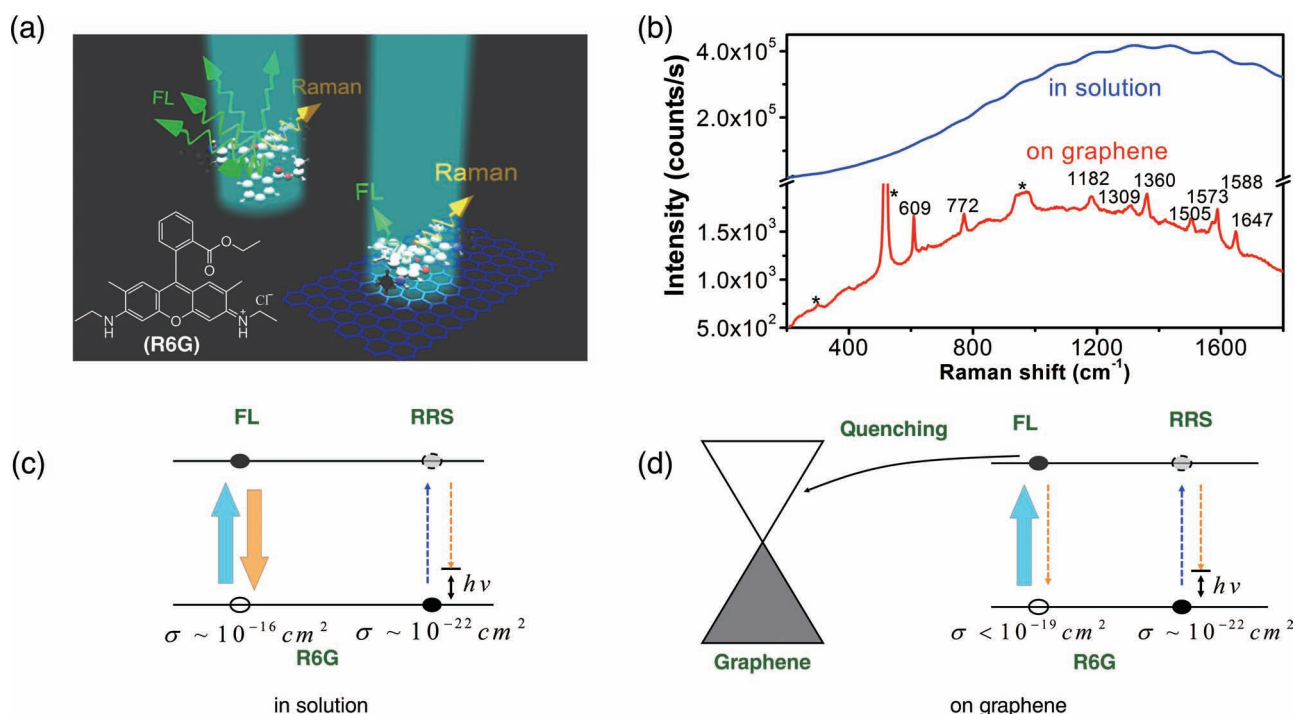
Figure 5. The fluorescence quenching effect of molecules adsorbed on graphene. a) The schematic diagram of graphene as a substrate for quenching fluorescence of R6G molecules. b) Comparison of Raman spectra of R6G in water (10 µM) and on a 1L graphene at 514.5 nm excitation. "∗" marks the Raman signals of SiO_2/Si substrate. c,d) The estimated photoluminescence cross-section of R6G in solution and on graphene, respectively. Reproduced with permission.[72] Copyright 2009, American Chemistry Society.

when treated with organic solvents.[79] These bands were assigned to some unknown organic matters contained in the Scotch tape which was used for the exfoliation of graphene. However, no clear Raman signals were found for regions with the residue on a SiO_2/Si substrate. It was thus speculated that graphene might have a Raman enhancement effect for the trace amount of residue matter. Systematic GERS experiments using dyes as Raman probes were then implemented,
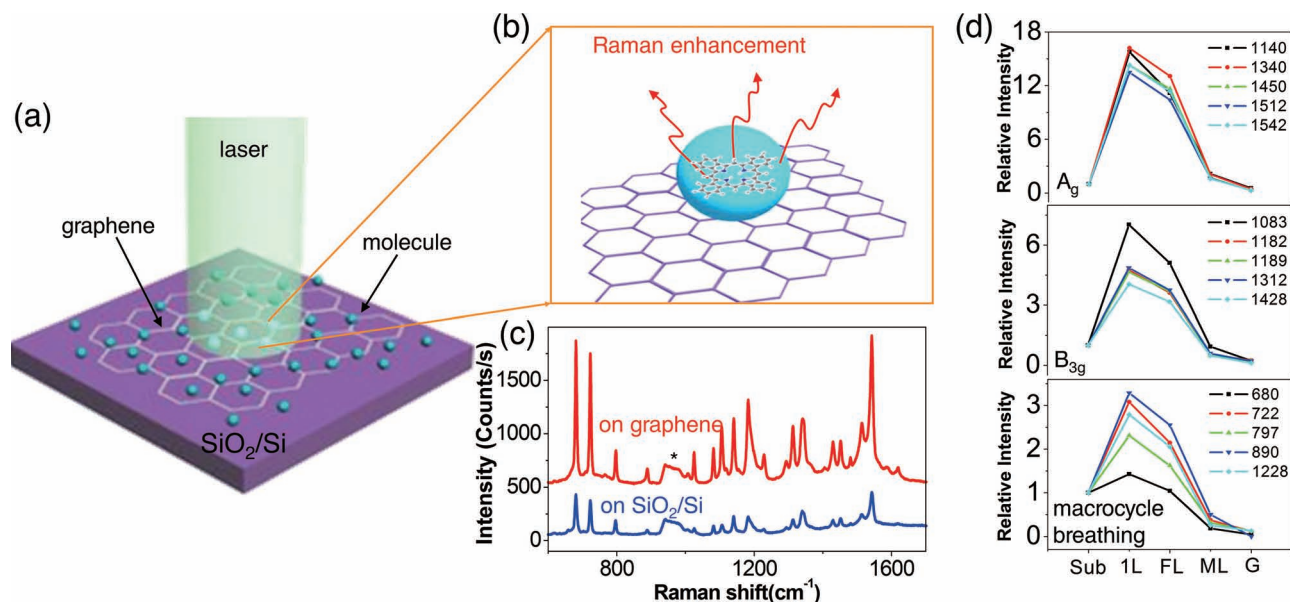

Figure 6. The GERS effect. a,b) Schematic illustration of the molecules on graphene and a SiO_2/Si substrate, and the Raman experiments. c) Comparisons of Raman signals of phthalocyanine (Pc) deposited on graphene (red line) and on the SiO_2/Si substrate (blue line) using vacuum evaporation (thickness 2Å) at 632.8 nm excitation. "∗" marks the Raman signals of SiO_2/Si substrate. d) The relative Raman intensity of Pc deposited on different surfaces using vacuum evaporation (thickness 2Å). The different spectral lines represent the different peaks of Pc labeled in the right top corner. The signals on the SiO_2/Si substrate are set to "1". Reproduced with permission.[78] Copyright 2010, American Chemistry Society.

including R6G, crystal violet (CV), phthalocyanine (Pc) and PPP, all of which are commonly used SERS probes.

Influence of the interference effect in GERS was also studied and this contribution was ruled out for the evaluation of GERS enhancement.[80] By fabricating series of SiO₂/ Si substrates with different thicknesses of oxide layers, Ling et al.[80] found that the intensity of GERS signals varies with the oxide layer thickness d, and the variation tendency is the same as molecules adsorbed on the SiO₂/Si substrate without graphene. This indicates that the presence of a thin layer of graphene (bilayer in our experiments) causes no observable variance in the interference phenomenon, and thus allows us to study the GERS enhancement directly with the interference effect ruled out.

The vibrational mode dependence of GERS is also investigated. GERS enhancement for bands of Pc with different symmetry (A_g, B_{3g} and macrocycle breathing vibrations) is summarized in Figure 6d,[78] the enhancement factor obeys the following order: A_g (~15 times)> B_{3g} (~5 times)> macrocycle breathing (~2 times). Despite the fact that GERS enhancement factor are relatively low (less than 10^2), Ling et al. found the detection limit of GERS can be as low as 8×10^{-10} M for R6G solution and 2×10^{-8} M for PPP. These results are comparable with SERS detections with a conventional noble metal substrate, and it is assumed that a considerable molecular enrichment effect should exist, possibly through π-π interactions.

Considering that the graphene substrate has several important advantages, such as uniformity, reproducibility, cleanliness and low detection limit for aromatic dyes, GERS is applicable in both fundamental studies of the SERS effect and many practical fields.

3.1.3. GERS Effect in Graphene Oxide, Graphene Edges, Graphene Quantum Dots and Meshed Graphene

Since the absence of electromagnetic contribution, graphene does not fit the traditional definition of a SERS substrate made of plasmonic materials. Chemical enhancement is considered to be the origin of GERS (will be discussed later). This leads to an interesting phenomenon that the GERS enhancement should be highly relevant to the chemical structure of graphene. Actually, the GERS effect for graphene in other forms have also been explored, such as GO,[81,82] graphene quantum dots (0D graphenes),[83] graphene edges,[84] and meshed graphene.[85] All of these graphene structures contain defects, e.g., GO is also in a layered structure (usually exfoliated from graphite oxide), which may contain –C–OH, –C–O–C–, and even –COOH groups. Since electronic state is a critical factor in chemical mechanism (and it is sensitive to defects in graphene), investigations on these kinds of defect-containing graphenes can help us understand the mechanism of the GERS effect. However, the current observations seem controversial. For instance, Yu et al. designed systematic experiments to investigate the enhancement factor of GO under different reduction time,[82] they found that increased reduction time causes a monotonous decrease in GERS activity, which indicates the important role of terminal groups in graphene–molecule interactions. Similarly, detailed fluorescence and Raman behavior of R6G on graphene antidot

superlattices were studied by Begliarbekov et al.,[86] in this case, the edges of graphene were also reported to be beneficial for improved Raman enhancement (and even stronger fluorescence suppression). Liu et al.[85] fabricated graphene nanomesh (through a local catalytic hydrogenation process by Cu nanoparticles, which was spontaneously p-doped), and observed an increased Raman enhancement on Rhodamine B (RhB). Local charge transfer and possible additional adsorption were reported to be responsible for these results. On the other hand, while in Wang et al.'s results,[84] they found that edged graphene (fresh samples prepared by mechanical exfoliation) is SERS-inactive for R6G, and the activity can be 'recovered' after annealing in vacuum. Consistent with their AFM observations, it is anticipated that the removal of residues on the graphene edges is responsible for this thermal-activation process.[84]

Since the complexity of the chemical enhancement mechanism, there has not been a universal model to describe the structure-dependent GERS response of graphene. When such a relationship is concerned, all of the following factors should be taken into careful consideration: intrinsic properties of the probe molecule, the molecule–graphene distance, energy band variation, doping, adsorption properties, as well as the excitation conditions.

3.2. GERS with a Chemical Enhancement Mechanism

The controversial origin of the huge SERS enhancement is an intriguing topic. The well-known EM (electromagnetic mechanism)/CM (chemical mechanism) debate has lasted for decades. Presently, it is widely accepted that for the Raman signals of molecules adsorbed on a rough metal substrate, the total SERS enhancement consists of two parts, i.e., a dominant EM contribution[87] and a minor CM contribution.[88,89] For the EM contribution, when the incident light is focused on a rough nanostructured metal substrate, the localized surface plasmons on the surface is excited, along with remarkably enhanced localized electromagnetic field in the vicinity of the metal nanostructure (so called hot spot), as a result, the Raman intensity of the molecules located close to nanostructure is enhanced by up to eight orders of magnitude or more.[90] For the CM contribution (also sometimes called the charge transfer mechanism), it is generally considered to be the result of the electronic coupling between molecules and the substrate.[10] During the past 30 or more years' development of SERS, the chemical contribution is generally nebulous, at least not as clear as the electromagnetic contribution. For the later, despite that both theoretical and experimental approaches towards quantum plasmonics are developing,[91] most electromagnetic field problems (particularly for particles larger than 10 nm) can be addressed by solving the Maxwell's equations, which obey the classical electrodynamic descriptions.

In most SERS systems, the relatively weak CM contribution coexists with the dominant EM contribution, and it is really a challenge to investigate the chemical contribution separately from the strong EM background. Furthermore, as CM enhancement is related with the molecular

© 2013 Wiley-VCH Verlag GmbH & Co. KGaA, Weinheim

level interactions, the surface roughness on the nanoscale for a normal SERS substrate is troublesome, both because of random molecular orientations and irregular molecular distribution.

Despite the fact that graphene plasmonics[92] is an area with growing interest, currently the GERS effect is considered to be absent of EM contribution. It is partly because of that the optical absorption of graphene is only about 2.3%, and the intrinsic graphene plasmon is in the THz frequency region that is far from visible (since the pretty low electronic density of pristine graphene). In GERS, molecules adsorbed on graphene surface offers a pure system for the investigation of CM enhancement. Considering that the graphene substrate has several aforementioned advantages, GERS is applicable for fundamental studies of the chemical effect of SERS. According to many theories which have been developed for describing the chemical mechanism for SERS study with metal substrates, herein, we examined the first layer effect, Fermi level modulation and wavelength-scanned experiments in GERS. Our results indicate that, all these characteristics thought to be typical features of CM effect in metal substrates do exist in a GERS process.

3.2.1. First Layer Effect in GERS

The first well-known feature of chemical enhancement in SERS is the short-range effect (also called the "first layer effect"). A close distance (i.e., direct contact) is necessary for a considerable CM enhancement. Since the beginning of the CM&EM debate in the earlier time soon after the SERS effect was discovered,[1,2] first layer effect was widely used as a proof of chemical enhancement mechanism.[93]

Now, the Raman enhancement on a graphene surface appeared to be especially suitable for the investigation of first layer effect (**Figure 7**a). In Ling et al.'s experiments,[94] self-assembled monolayers of PPP prepared by the LB technique were selected as the probe molecules. On one hand, 0, 1, 2, 3, 4-monolayers of PPP on the bare SiO_2/Si substrate, with graphene on the top and with graphene on the bottom were constructed. Raman investigations showed that the GERS intensity of PPP is clearly distance-dependent. The first layer next to graphene contributed the dominant part of Raman intensity and there was almost no observable additional

enhancement since the third layer. On the other hand, interestingly the GERS enhancement was found to be sensitive with the molecular orientation of PPP. PPP is an asymmetric molecule with two ends, i.e., the –COOH side (the carboxyl group) and the –CH=CH2 side (the vinyl group). Two configurations of graphene/PPP combined structure can be fabricated, with either the –COOH side or the –CH=CH2 side contacted with graphene. Distinguished GERS enhancement property for the two configurations was observed. Detailed vibrational assignments indicated that a stronger GERS enhancement occurs when the related functional group is closer to the graphene surface. Furthermore, as a symmetric molecule, CuPc (copper phthalocyanine) was used for the reference experiments. The Raman enhancement behavior of graphene/CuPc showed no observable differences for the two configurations.

3.2.2. Fermi Level Modulated GERS Enhancement and Wavelength Scanned Excitation Profile of GERS

According to the charge-transfer model of chemical contribution in SERS, the enhancement can also be considered as a modified resonance effect (because of the formation of charge-transfer states) and the enhancement is related with the Fermi level of the metal. Similarly, for a considerable GERS enhancement, it requires an energy match between the energy levels of probe molecules (highest occupied molecular orbital, HOMO; and lowest unoccupied molecular orbital, LUMO) and the Fermi level of graphene. Actually many experimental results in electrochemical systems have confirmed this statement for metal substrates.[95,96] For the case of graphene, as a semimetal with a zero band gap, its Fermi level can be modulated by adding a positive or negative gate voltage (Figure 7b). Systematic experiments were designed towards a deeper understanding on the charge transfer effect. A series of metal phthalocyanine (M-Pc) molecules (M = Mn, Fe, Co, Ni, Cu, Zn) with different molecular energy levels were used as probe molecules, and their GERS enhancement performance under different gate voltages was investigated.[97] It was found that, for all the M-Pc molecules investigated, a positive gate voltage (an up-shifted Fermi level) resulted in a decreased GERS enhancement, and oppositely, an increased GERS signal was observed when
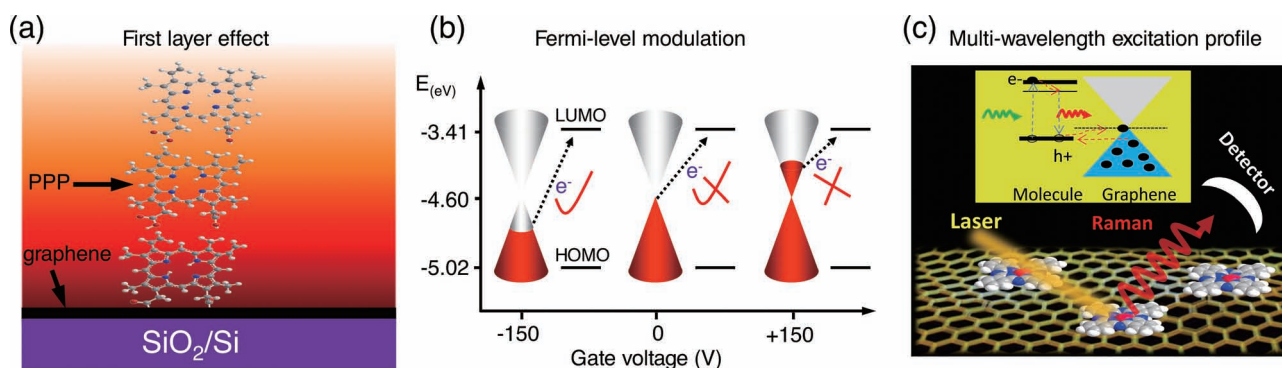

Figure 7. Chemical mechanism based features of GERS. a) First layer effect in GERS. Reproduced with permission.[94] Copyright 2010, Wiley-VCH. b) Fermi-level modulation of GERS. Reproduced with permission.[97] Copyright 2011, American Chemistry Society. c) Wavelength-scanned excitation profile of GERS. Reproduced with permission.[100] Copyright 2012, American Chemistry Society.

a negative gate voltage was applied (a down-shifted Fermi level). For excitation with a fixed wavelength, the Fermi level modulated response of GERS enhancement means changed resonance energy for M-Pc molecules on graphene. In this method, the Fermi level of graphene can be modulated from –4.98 eV to –4.22 eV, and a larger gate voltage may cause electric tunneling effects for a 300 nm thick SiO$_2$ insulating barrier. It is anticipated that the electrochemical system may give a larger Fermi level modulation range, yet a carefully designed sample structure is required. As also was discussed in the Raman spectrum of graphene (in Section 2.1), besides electric gate doping, chemical doping effect is also prominent in GERS. During the above measurements, the device was exposed to the atmosphere and there was always a hysteresis effect cause by the adsorbed dopants. A fast sweep rate is essential for the observation of GERS enhancement modulation. Further investigation under vacuum and an n/p-doping atmosphere (NH$_3$ and O$_2$) confirmed this assumption.[98,99]

Besides the Fermi level modulation of the substrate, the charge transfer mechanism based GERS enhancement can also be modulated by the energy of incident laser. Wavelength-scanned Raman excitation spectroscopy is useful to scratch the wavelength-dependent excitation profile, and then the detailed charge transfer model can be studied. To investigate the details of the GERS effect, wavelength-scanned Raman excitation experiments were carried out (Figure 7c). Raman excitation profiles of the CuPc molecule were obtained in the range of 545~660 nm, the results suggested that the GERS enhancement herein obeys a ground-state charge transfer model.[100]

From the above, we can find that GERS enhancement is sensitive to the molecule-graphene distance, molecular orientation, electronic energy levels of both graphene and the molecules, and incident conditions. All these are common characteristics consistent with the chemical enhancement in noble metals. Thus, results will be case-dependent when discussing whether a GERS enhancement effect exists or the evaluation of its enhancement factor. Things may be more complicated at the presence of fluorescence, for example, Brus et al.[101] reported a decreased Raman cross-section of R6G on graphene under 514.5 nm excitation (based on a series of approximations). Direct Raman investigations on a larger class of GERS cases will allow us to better understand the GERS effect.

3.3. GERS for Applications in Probing the Molecular Orientation

The manifold superiorities of GERS impact itself the capacity for some fine applications, for example, probing molecular orientation. Studying the relationship of molecular orientation and SERS enhancement performance is an important but always troublesome project. Main difficulty is that we can hardly control the molecular orientation and their amounts on a rough SERS substrate. Graphene has an atomically flat surface, which enables Raman enhancement measurements of molecules with more controllable states. For example, Ling et al.[102] studied the GERS behavior of a CuPc monolayer on

graphene during a thermal annealing process. The variation of Raman intensity of the CuPc monolayer with increased temperature (from room temperature to 600 °C) is interesting. As for the SiO$_2$/Si substrate without graphene, a monotone decreasing signal was observed. While for the graphene/SiO$_2$/Si substrate, the signal largely increased at first, reached at a maximum at around 300 °C and then it decreased. To understand this phenomenon, we proposed the following transformation process: pristine CuPc monolayer prepared by the LB technique is in an upstanding orientation; during the heating process, CuPc molecules become partially sublimated, and the rest molecules on the substrate tend to transform to a lying down orientation. Continued heating sublimates more molecules. These speculations were further confirmed by AFM characterization results. Thus these observations are vigorous proofs of an orientation-dependent GERS enhancement, a lying down orientation is essential for a considerable GERS enhancement (since this configuration for planar CuPc matches graphene substrate better). Furthermore, an estimated CM enhancement factor of 43 was acquired, which was larger than our earlier reported results (2~17[78]). Similarly but more interestingly, the thermal annealing behavior of a PbPc (unlike CuPc, it is non-planar) monolayer was also monitored, the upstanding to lying down transformation, the non-planar to planar deformation, and the reduction of Pb(II)Pc to Pb(0)Pc processes were observed.[103]

4. Graphene-Containing Composites towards SERS Substrates with Improved Performance

Obviously, the dominant contribution of SERS is electromagnetic enhancement, which is the primary reason that imparts SERS its capacity for ultra-sensitive detection down to the single molecule level. In a GERS substrate, the absence of electromagnetic enhancement simplifies the investigation of the chemical mechanism in SERS, but simultaneously, it causes a considerable loss of sensitivity.

Besides GERS, many researchers are developing graphene-involved metal substrates for SERS.[49,64,104–126] As a new kind of additive, graphene is a multi-functional improving agent in many graphene-based composite substrates for SERS. Typical functions including: surface passivation, surface enrichment, additional chemical enhancement, fluorescence quencher, internal label, and so on.

4.1. Graphene as a Spacer for Surface Passivation

Among various characterization technologies, as the sensitivity increases, the requirement on a lowest inner disturbance from the analytical tool becomes more important. During the past decades, most SERS experiments are limited to cases with molecules exposed to a bare metal surface. While the gold and silver are natural catalysts for many kinds of oxidation/reduction reactions, making SERS substrate also a seedbed for various chemical interactions (even reactions). Main unfavorable disturbances including chemical adsorption-induced vibrations, charge transfer between the metal

and molecules, photo-induced damage and metal-catalyzed side reactions, etc. As a result, the information from a SERS spectrum is always mixed with substrate-induced disturbances (due to metal–molecule interactions) and would no longer clearly dependent on the primary structure of analytes.

4.1.1. Metal–Molecule Isolation

The concept of surface passivation was then proposed. In a passivated SERS substrate, a thin and pinhole free coating layer is used to prevent metal–molecule contact. Such a coating layer serves as an inert shell, which can be made of Al_2O_3,[11,127] SiO_2,[11,128] diamond-like carbon[129] and graphene.[64,65] These approaches are called as shell-isolated SERS. Fabrication of a passivated SERS substrate at a lowest loss of electromagnetic enhancement activity is the key of shell-isolated SERS. The inert shell should have a very small thickness (to prevent substrates from apparent loss of the electromagnetic enhancement activity), yet it should be pinhole free (to thoroughly isolate the metal–molecule contact and thus prevent possible undesirable interactions).

Towards such a thin and seamless inert shell, so far atomic layer deposition (ALD) (preparation of Al_2O_3),[11,127] wet chemistry methods (preparation of SiO_2),[11] and physical vapor deposition method (preparation of a diamond-like carbon film)[129] have been explored, with improved SERS performance. For example, Zhang et al. showed that an Al_2O_3 layer can make the silver substrate much more stable (with a shelf-time longer than 9 months).[127] Systematic experiments on shell-isolated SERS with the concept of metal–molecule isolation were reported by Tian's group,[11] who first demonstrated a series of measurements which would be challenging with a normal metal substrate. For example, SERS signals of Pt-H vibration with intrinsic frequency were acquired with either SiO_2-shelled or Al_2O_3 shelled gold nanoparticles, while the bare gold nanoparticles caused self-induced down-shifts from spontaneous charge transfer (due to the different work functions between Au and Pt, 5.10 eV for Au and 5.65 eV for Pt, respectively).[11] In this section, we will focus on the discussions of how graphene becomes a suitable candidate for the extended developments of shell-isolated SERS.

4.1.2. Graphene Passivates the Metal Substrate

According to the above-mentioned key points, the unique structure (the atomic thickness, seamless structure and chemical inertness) of graphene makes it a natural candidate material for shell-isolated SERS. Despite that the practicability sounds to be obvious, yet the performance of graphene-shell-isolated SERS substrate is doubtful. Actually, Liu et al. think the pristine conductive graphene may screen the enhanced electric field from the underlying silver substrate, and they designed a hydrogenation process (induced by H_2 plasma treatment, which will largely reduce the conductivity of graphene) to improve the sensitivity of graphene-coated silver substrate.[109] SERS-activity of a pristine and hydrogen-terminated graphene covered silver nanoparticle substrate was investigated in comparison, and according to their observations, Liu et al. proposed that the hydrogenation process is beneficial for a stronger SERS activity due to a smaller screening effect of the localized electric field. However, both experimental and theoretical results have shown that the graphene layer does not cause the electric field to decay obviously.[64,130] To verify that whether the presence of a graphene shell works for a passivated SERS with acceptable sensitivity, rationally-designed experiments were implemented. In our experiments, graphene-covered regions and bare metal regions were fabricated at the same time and their Raman features were compared in detail. We found that, the graphene shelled substrate provides a cleaner baseline unlikely to suffer from photo-induced damages such as photo-carbonization and photo-bleaching. More interestingly, fluctuation among substrates with different material/morphology is always a famous characteristic of SERS, while things are different for a graphene-shell-isolated SERS substrate. As shown in **Figure 8**, graphene-shell-isolated substrates with both gold and silver as an electromagnetic enhancer showed highly consistent results for R6G, while inconsistent results (with shifted or some new emerging features, yet they are irreproducible) were observed when bare gold or silver substrate was used.[64] In addition, varied SERS features of CuPc using an 8-nm gold film before and after annealing was also observed, while this difference could be brought down with a graphene shell.[65] It is found that the graphene shell tends to play an important role in the final spectral feature, in a sense, graphene-shell-isolated SERS is the electromagnetically enhanced GERS, in which the huge EM enhancement is introduced, meanwhile an chemically inert surface is reserved.

4.2. Molecular Enricher for Aromatic Analytes

The second important role of graphene in a composite SERS substrate is molecule enrichment. The prominent position-sensitive property of SERS requires a short substrate-molecule distance for a huge SERS enhancement. A good affinity between the SERS substrate and the analytes is essential to bring the analytes in close proximity to the substrate. Thus, for most cases, the existence of possible driving forces that enable spontaneous surface adsorption of analytes onto a certain SERS substrate is also an important consideration.

4.2.1. Driving Forces for Surface Adsorption

There are many forces which are effective for spontaneous adsorption of molecules on a metallic SERS substrate. First is surface bonding, such as the formation of metal-sulfur bonds for thiols and the surface coordination bonding for nitrogen-containing compounds. Second important kind of force is electrostatic attraction. For instance, colloidal metal nanoparticles prepared through the reduction by citrates are usually negatively charged and thus tend to have more intense interactions with positively charged molecules, such as CV. Actually, in many cases these driving forces are absent, and then spontaneous adsorption does not occur. This will cause trouble especially for SERS analyses in colloidal systems or samples prepared by the solution-soaking method. In such cases, we may be required to prepare samples through a drop-drying process. A better molecule generality is desired to push forward the wider applications of SERS.
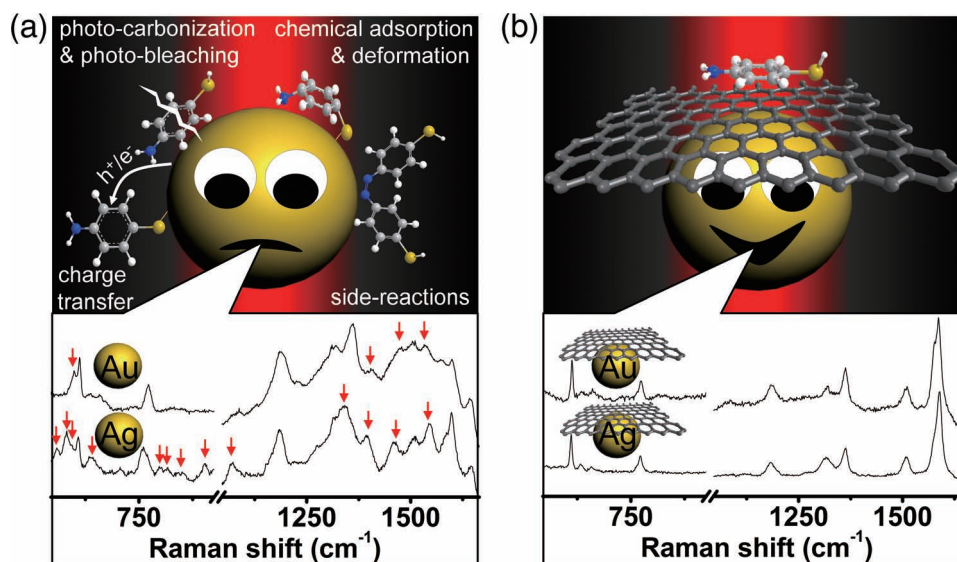
Figure 8. Surface passivation of metal substrate for SERS with graphene. a) Normal SERS with various possible metal–molecule interactions. Au and Ag show different SERS features of R6G, as marked by red arrows. b) Graphene-shell-isolated SERS. The presence of graphene layer brings down the difference of metal enhancer, which shows same Raman features of R6G for Au and Ag. Vacuum thermal evaporated metal nanoislands were used as the electromagnetic enhancer, and all spectra were taken with the same conditions. Spectral data adapted with permission.[64] Copyright 2012, National Academy of Sciences.

4.2.2. Graphene as a Molecule Catcher via π–π Interactions

As a single sheet of sp^2 carbon atoms, the delocalized π-bond of graphene acts as a natural "magnet" for collecting aromatic molecules. Since a large class of probe molecules in SERS are aromatic, π-π interactions of graphene-molecule can serve as a new driving force for surface adsorption, which is inaccessible for a conventional metallic SERS substrate.

For example, Liu et al.[111] demonstrated that GO functionalized with silver nanoparticles for ultrasensitive detection of aromatic molecules with various charges, such as crystal violet (CV) with positive charge, amaranth with negative charge, and neutral phosphorus triphenyl (PPh3). Similarly, in Lu et al.'s experiments, Ag/rGO and Au/rGO composites were prepared and detection limit of several aromatic molecules on the nM level was achieved.[112]

Nevertheless, in some cases π-π interaction is not the only driving force of graphene in graphene-involved SERS substrates. For instance, Ren et al.[113] fabricated positively charged GO (hybridized with silver nanoparticles) functionalized with poly(diallyldimethyl ammonium chloride) (PDDA), for detection of folic acid (which is negatively charged) both in water and serum. Detection limit down to 9 nM was realized, with a linear response range from 9 to 180 nM. It should be noted that, graphene itself is also an ideal model for various kinds of functionalization.[131] Well-designed functionalization can be exploited for SERS detection with certain kind of adsorption force (besides π-π interaction), both physically and chemically. For example, the influence of defects in Raman enhancement of graphene for pyridine was investigated theoretically in Kong et al.'s results by density functional theory.[120] In such cases both the enrichment effect of molecules and their chemical interactions with the modified graphene should be taken into consideration.

4.3. An Additional Chemical Enhancer

Again, the chemical enhancement of graphene is discussed in graphene-metal composite SERS substrates. There have been quite a few works in which graphene was explored for SERS detection with improved sensitivity, and rather than a molecular enrichment, in some papers this effect was assigned to be an additional chemical enhancement.[115,130] For example, in Hao et al.'s experiments,[130] patterned gold nanohole and nanoparticle arrays (prepared by electron beam lithography, EBL) were transferred with CVD-grown graphene, resulting in a combined structure. By comparisons on different sample regions, they reported that the graphene-coated region has a 3-fold (for nanohole array) and 9-fold (for nanoparticle array) additional SERS enhancement. In their discussions, this additional enhancement was attributed to an additional CM enhancement from graphene.

However, we should realize a fact that, the discussion on detailed contribution of molecular enrichment or additional CM enhancement would be valid only when the amount of molecules can be precisely identified. Yet this is a pretty hard issue, partially due to the self-complexity of the SERS system. So far the contribution of molecule enrichment effect and additional CM enhancement is still unclear. To address this problem, more detailed parallel studies and a cleaner analytical system may be preferred. Despite of this uncertainty, the existence of graphene does contribute to a stronger SERS signal, it is still a desirable way to be exploited for ultrasensitive SERS detections.

4.4. Other Effects

Besides the aforementioned aspects, graphene, as a multifunctional improving agent, it does work in many other

aspects, such as fluorescence quencher, internal label and related.

First is as a fluorescence quencher. Similar to the case of a pure graphene substrate without metal, the fluorescence quenching effect is also prominent for probe molecules in a graphene-involved composite SERS substrate. Interestingly, graphene is found to be an effective fluorescence quencher, both for the probe molecules and the metal substrate. The quenching effect for fluorescent dyes is similar to the case which we have discussed in GERS. Furthermore, a fluorescent background usually occurs in a metallic SERS substrate itself. Wang et al.[108] reported that gold on graphene shows a lower fluorescence background than gold on the SiO$_2$/Si substrate. In our work, double layer graphene covered gold film was fabricated and in-situ monitoring during a thermal annealing process was carried out, a consistent lower fluorescence background was observed for the whole temperature range (from room temperature to 400 °C). Dynamic evolution process indicated that the contact state of gold/graphene is essential for a considerable quenching effect.[65]

Second is as an internal label. Quantitative analysis is one of the most desirable potential applications of SERS. Selection of a good internal label is half way to the success towards a reliable quantitative result. Interestingly, graphene integrates all-sided aspects that an ideal internal label should have. Particularly, the atomic uniformity, chemical inertness and the clean and characteristic Raman signal of graphene make itself a unique and natural internal label. This role will be more appealing when the SERS substrate is flat (as will be discussed in the following section). Towards this goal, more efforts are remaining to be paid, and it is expected to see some substantial breakthroughs in the near future.

For other functions, we believe there is plenty of space waiting for further exploitation. Better use of graphene will enable us to better understand the SERS effect, better handle the SERS technique, and better extend SERS for practical applications.

5. SERS on a Flat Surface: Design, Fabrication, and Applications

SERS is a powerful tool and it can be more powerful when exploited with a carefully designed substrate. For example, thought SERS substrate as a knife, the primordial rough SERS substrate is strong enough to cut anything into irregular oddments, and researchers are trying their best to design knives with sharper and smoother edges for finer craft.

According to the origin of the localized surface plasmon resonance effect, considerable electromagnetic enhancement is only limited to metal substrate with highly curved or gapped nanostructures. A satisfying solution towards the dream of doing SERS on a flat surface has become a long-term issue. With the utilization of graphene as a building block, SERS measurement with localized electromagnetic hot spots on an atomically flat surface for SERS is no longer untouchable.

5.1. Design and General Considerations

Roughness is widely accepted to be a critical premise where a strong SERS effect happens. However, for many analytical situations, a flat SERS substrate is highly preferred. Actually, the pursuit of doing SERS on a flat surface has been already put on the agenda. Earlier attempts like research works of SERS experiments on a single crystal surface[132,133] (including the GERS effect found recently[78]) do realized SERS enhancement (but only chemical enhancement) on an atomically flat surface. Yet the absence of EM enhancement has ruled out this method in most practical applications. TERS[134,135] is another choice. The SPM tip serves as a 'mobile' hot spot, and it is capable for SERS investigation of adsorbates on a smooth surface. The drawbacks lie in both the complicated equipment and relatively low enhancement efficiency (even fluctuant TERS response) from hot spot of a single tip. Spreading a layer of SERS active metal nanoparticles onto the target flat surface is alternative way of magnified TERS (increased amount of hot spots), but in this case self-contamination from the metal nanoparticles and solvents becomes inevitable. While now, the rise of graphene offers us another choice.

The unique structure and properties, i.e., a perfect two-dimensional crystal which is atomically smooth, atomically thin and chemically inert, make graphene an ideal building block of a flat SERS substrate. As shown in **Figure 9**b, a new combined substrate consisting of SERS active metal and
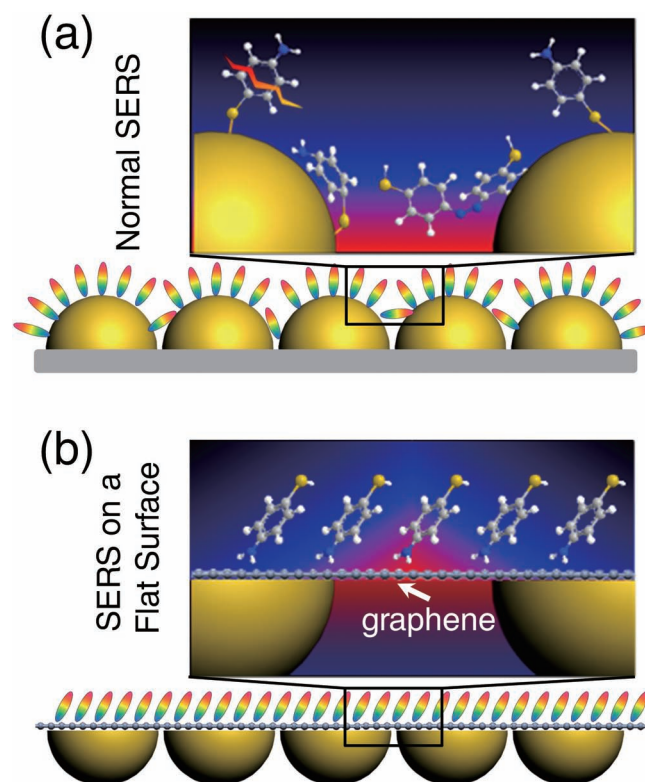

Figure 9. Schematic illustration of (a) molecules on a normal SERS substrate and (b) molecules on flat SERS substrate mediated by a flat graphene surface. Reproduced with permission.[64] Copyright 2012, National Academy of Sciences.

graphene was designed to do SERS on a flat surface. In a combined substrate, the electromagnetic enhancement from roughened/nanostructured SERS metals was 'mediated' by a flat graphene layer (referred to as graphene-mediated SERS, G-SERS). The possible behaviors of molecules adsorbed on a normal SERS substrate (Figure 9a) and on a flat SERS substrate (Figure 9b) mediated by graphene are illustrated. On one hand, the graphene layer serves as an atomically flat supporter for more controllable molecular arrangement; meanwhile, it separates the metal–molecule contact and thus rules out possible disturbances induced by metal–molecule interactions. This is an effective approach to cut down the morphology/material-induced complexity of a SERS system.

Besides the considerations on graphene (the SERS mediator), the morphology of SERS-active metal (the electromagnetic enhancer) is also not arbitrary. In order to make the electromagnetic hot spots to be collected on a flat graphene surface, there is a general rule that, the arrayed nanostructures must form arrayed hot spots next to the planar graphene surface. For example, an array of hemi-spheres (with the flat side contact with graphene) is much more desirable than that of spheres. In our experiments, gold and silver nanoislands prepared by vacuum thermal evaporation were exploited to fabricate such flat substrates.[64] The practicability of substrates in this configuration was verified by both theoretical and experimental results.

First, 3D finite difference time domain (3D-FDTD) was carried out. Two 60-nm gold hemispheres were used to represent the island-like gold nanoparticles. By comparison on two systems for gold hemispheres with and without graphene, it was exciting to find, that the presence of graphene layer does not cause the electromagnetic field to decay, but oppositely provides an additional almost one-fold increase on the maximum $|E_{loc}/E_0|^2$. The following aspects were considered to be responsible for this phenomenon: 1) The atomic thickness of graphene guarantees negligible distance-dependent attenuation effect. This is important since the electric field of localized hot spots attenuates with the distance away from the central strongest point in an exponential way; 2) The high optical transparency of graphene. The absorption of monolayer graphene is ~2.3% and it is not supposed to cause obvious loss of incident intensity; 3) Graphene layer causes multi-scattering processes, results in a refocused light at the interface. Actually, similar effect of SiO_2-coated Au/Ag nanoparticles has also been reported by Xu et al.;[128] 4) A small screening effect and/or possible plasmon coupling effect of graphene on gold. Usually a metallic cover layer will screen the electric field of underlying substrate, while for the case of graphene, it is more like a dielectric media since its relatively low electronic density. Meanwhile, for graphene with designed doping/functionalization, the intrinsic plasmon frequency can be tuned, and considerable coupling is then in prospect.

Second, parallel experiments were designed to check the sensitivity of SERS on a flat graphene surface. A selected sequence (evaporation of molecules, then transfer of graphene, and finally evaporation of SERS-active metal nanoislands) was designed to ensure an equal amount of probe molecules (CuPc, here in our case) between the SERS

and G-SERS regions. The pristine, GERS, G-SERS(Au), SERS(Au), G-SERS(Ag), SERS(Ag) spectra of CuPc were acquired under the same conditions. Through comparison on the integrated area of the 1530 cm^{-1} peak, the pristine intensity is enhanced by a factor of 14 for GERS, 61 for SERS(Au), 85 for G-SERS(Au), 580 for SERS(Ag), and 755 for G-SERS(Ag).[64] This result showed that SERS on a flat surface is capable for ultra-sensitive detection with comparable (and even larger, for certain vibrational modes) enhancement factor as normal SERS.

5.2. Transparent, Flexible, and Freestanding Substrate with a Flat Surface: Fabrication and Applications

Besides the concern about sensitivity, reproducibility and selectivity, a desirable SERS substrate should be easy to be prepared, stored and operated. High sensitivity and selectivity are internal beauties of SERS by nature. Current efforts towards more reproducible SERS analyses are mainly focused on the tailoring or assembly of substrates with regular nanostructures,[136–139] which provide SERS signals with better uniformity. Besides, regular nanostructures would also benefit theoretical understandings of the SERS effect, since they can be described with a simpler model. The concept of shell-isolated SERS[11] is another revolutionary step, towards more intrinsic and reproducible signals free of fluctuations induced by metal–molecule interactions. These achievements are meaningful progresses but it is not a terminal point.

SERS on a flat graphene surface inherits the merits of both 'hot spot engineering' and metal–molecule isolation.[64] A 'universal' G-SERS substrate in a new form was developed for extended applications. In our recent work,[64] transparent, free-standing and flexible 'G-SERS tapes' were fabricated, towards quick, precise, non-invasive and ultrasensitive sensing, imaging and real-time monitoring applications for any target surface with any arbitrary morphology. As summarized in a recent perspective article by Liz-Marzán et al.,[12] flexible substrate has become a fashionable trend in SERS. As illustrated in **Figure 10**a, the transparent, flexible and freestanding G-SERS substrate consists of three parts: from bottom to top are the polymer supporter, the sandwiched metal enhancer and the top flat graphene mediator, respectively. This method is suitable for scalable production (Figure 10b), and atomic force microscopy (AFM) image shows the roughness of the as-prepared flat substrate is within ±2 nm (Figure 10c). Typical analyses are shown in Figure 10d. Apart from providing sensitive detection comparable as that provided by the normal SERS process, the new form of G-SERS substrate exhibits its own advantages.

As a new branch of green chemistry, green analytical chemistry[140] has become a priority area of analytical chemistry in recent years because of the rising environmental concerns and economical considerations. For almost all sorts of analytical methods, the dream to improve their sensitivity as well as their reproducibility and to optimize the analytical process (e.g., to simplify the sample preparation/measurement procedures for quick analysis and to enable in-situ and real-time monitoring) is a long-term pursuit. The standards to
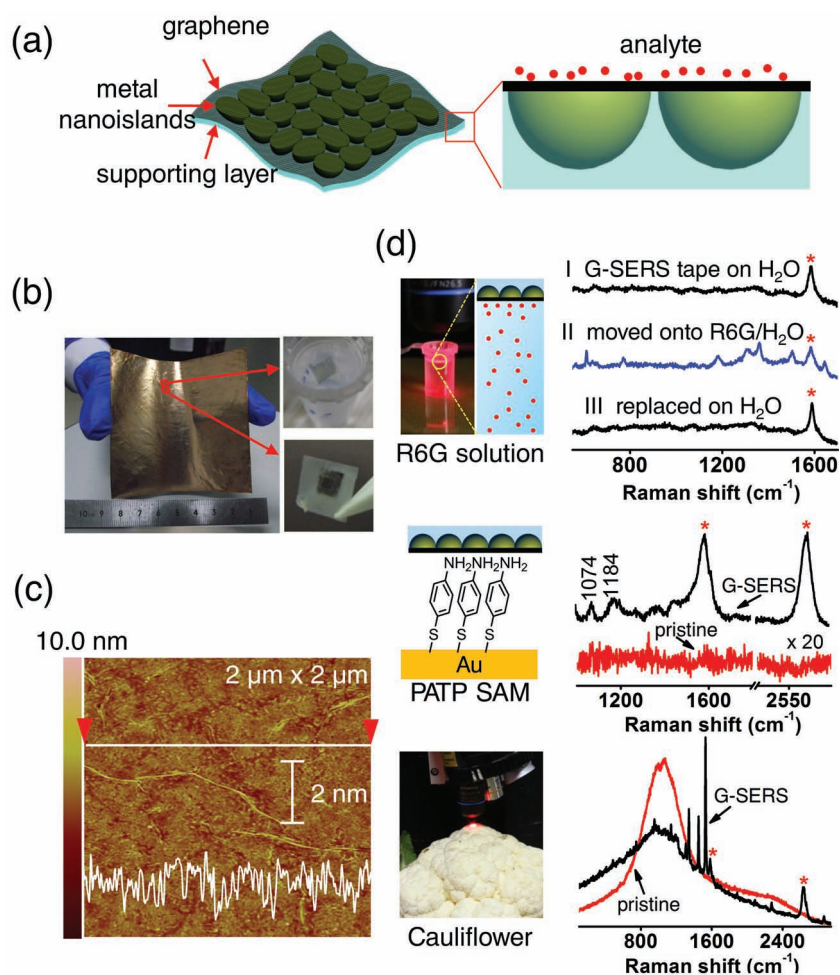
Figure 10. SERS on a flat surface in a transparent, flexible and freestanding form towards applications. a) Components of a G-SERS tape. b) Scalable production. Pictured is a photograph of an 8×8 cm^2 G-SERS substrate before the removal of copper. Insets on the right are two freestanding G-SERS(Au) tapes, one is floating on water (top) and the other is held with tweezers (supported by a windowed scotch tape) (bottom), respectively. c) Atomic force microscopy (AFM) image shows the roughness of the as-prepared flat substrate is within $\pm$ 2 nm. d) Typical analyses with a G-SERS(Au) tape. Top: a real time and reversible G-SERS characterization of R6G directly in a 1×10^{-5} M aqueous solution. (I, II, III are the Raman spectra with the same G-SERS tape on H$_2$O, R$_6$G/H$_2$O and replaced on H$_2$O); Middle: pristine (red line) and G-SERS (black line) measurements of a self-assembled monolayer (SAM) of p-aminothiophenol on a flat gold surface; Bottom: pristine (red line) and G-SERS (black line) measurements of a cauliflower surface with adsorbed CuPc (by soaking in a 1×10^{-5} M CuPc solution in ethanol for 10 min). "∗" marks the enhanced G-band and G'-band features of 1LG. Reproduced with permission.[64] Copyright 2012, National Academy of Sciences.

guarantee an analytical process to be 'green' have been listed in reference.[140–143] For the case of SERS with a G-SERS substrate, possibly there are following characteristics that can be considered as a 'greener' analytical process: 1) G-SERS tape allows direct measurement of analytes on any arbitrary surface, which is almost free of sample preparation, with good compatibility for analytes in various states; 2) Metal nanostructures encapsulated in a G-SERS tape are isolated with the atmosphere, thus a G-SERS substrate is anticipated to have long-shelf time without evident decrease on enhancement activity, which will be helpful in practical applications that one may not need to prepare a SERS substrate before

doing a SERS measurement; 3) Since the metal–molecule isolation, a G-SERS substrate is confirmed to provide cleaner and more reproducible signals, which will benefit a quicker data analysis procedure; 4) A G-SERS substrate provides an atomically flat surface for Raman enhancement, thus makes it less challenging to arrange molecules in controlled amounts and definite orientations, by virtue of taking the Raman signal of monolayer graphene as a natural internal standard, it is anticipated that precise and more efficient quantitative SERS measurements can be easier to be realized on a G-SERS substrate. 5) The encapsulated structure of metal nanostructures in a G-SERS tape also allows obtaining signals without contaminating samples, making G-SERS analysis a non-invasive process; 6) As demonstrated in Figure 10d, use and reuse tests of a G-SERS tape show that G-SERS tape is reusable with no residues, which suggests G-SERS to be an economized way of saving resources (mainly noble metals).

From the above we see a transparent, freestanding and flexible G-SERS substrate for SERS analysis is capable for simpler pre-treatments, quicker data acquisition for reliable results, less contaminations and more economical. All of them are important aspects of a green analytical process and we thus anticipated that this kind of G-SERS substrate provides a 'greener' way to do SERS.

6. Conclusion and Outlook

Graphene, a candidate for next-generation integrated circuits,[144] does work well in SERS. Yet the application of graphene in SERS is not a random invention. It should be noted that, the roles of graphene in many cases work together, which makes it a multi-functional agent for the improvement of SERS. SERS experiments are being implemented in a more well-designed way. By the virtue of graphene's unique structure and physical/chemical properties, it has become an important material for SERS. In-depth studies on graphene-involved SERS are expected to offer deeper understandings of both the SERS effect (and other plasmon-related theories), as well as a better balance on sensitivity, reproducibility, and selectivity in the performance of SERS. Yet the capacity of graphene remains to be exploited and current progress is far from enough. The main challenges lie in the following aspects: controllable functionalization of graphene samples with intended functions; the design and integration of Raman probes, plasmonic metal structures, and other functional

materials; more reliable qualitative/quantitative evaluation of SERS experiments; more convenient/compatible SERS techniques. Beyond graphene, intentionally or not, other emerging materials may also bring SERS to a new stage. We are optimistic that in the near future SERS may enter (and change) our daily lives.

Acknowledgements

[1] M. G. Albrecht, J. A. Creighton, *J. Am. Chem. Soc.* **1977**, *99*, 5215–5217.

[2] D. L. Jeanmaire, R. P. Van Duyne, *J. Electroanal. Chem.* **1977**, *84*, 1–20.

[3] K. Kneipp, Y. Wang, H. Kneipp, L. T. Perelman, I. Itzkan, R. Dasari, M. S. Feld, *Phys. Rev. Lett.* **1997**, *78*, 1667–1670.

[4] S. Nie, S. R. Emory, *Science* **1997**, *275*, 1102–1106.

[5] M. Fleischmann, P. J. Hendra, A. J. McQuillan, *Chem. Phys. Lett.* **1974**, *26*, 163–166.

[6] M. J. Natan, *Faraday Discuss.* **2006**, *132*, 321–328.

[7] X. M. Lin, Y. Cui, Y. H. Xu, B. Ren, Z. Q. Tian, *Anal. Bioanal. Chem.* **2009**, *394*, 1729–1745.

[8] B. Sharma, R. R. Frontiera, A. I. Henry, E. Ringe, R. P. Van Duyne, *Mater. Today* **2012**, *15*, 16–25.

[9] X. Gong, Y. Bao, C. Qiu, C. Jiang, *Chem. Commun.* **2012**, *48*, 7003–7018.

[10] A. Otto, M. Futamata, *Top. Appl. Phys.* **2006**, *103*, 147–182.

[11] J. F. Li, Y. F. Huang, Y. Ding, Z. L. Yang, S. B. Li, X. S. Zhou, F. R. Fan, W. Zhang, Z. Y. Zhou, D. Y. Wu, B. Ren, Z. L. Wang, Z. Q. Tian, *Nature* **2010**, *464*, 392–395.

[12] L. Polavarapu, L. M. Liz-Marzan, *Phys. Chem. Chem. Phys.* **2013**, doi: 10.1039/C2CP43642F.

[13] K. S. Novoselov, A. K. Geim, S. V. Morozov, D. Jiang, Y. Zhang, S. V. Dubonos, I. V. Grigorieva, A. A. Firsov, *Science* **2004**, *306*, 666–669.

[14] A. K. Geim, K. S. Novoselov, *Nat. Mater.* **2007**, *6*, 183–191.

[15] A. Gupta, G. Chen, P. Joshi, S. Tadigadapa, P. C. Eklund, *Nano Lett.* **2006**, *6*, 2667–2673.

[16] F. Tuinstra, J. L. Koenig, *J. Chem. Phys.* **1970**, *53*, 1126–1130.

[17] M. S. Dresselhaus, A. Jorio, R. Saito, in *Annual Review of Condensed Matter Physics*, Vol. *1* (Ed: J. S. Langer), **2010**, pp.89–108.

[18] A. Jorio, R. Saito, G. Dresselhaus, M. S. Dresselhaus, in *Raman Spectroscopy in Graphene Related Systems*, Wiley-VCH Verlag GmbH & Co. KGaA, Germany **2011**, pp.277–298.

[19] C. Thomsen, S. Reich, *Phys. Rev. Lett.* **2000**, *85*, 5214–5217.

[20] L. M. Malard, M. A. Pimenta, G. Dresselhaus, M. S. Dresselhaus, *Phys. Rep.* **2009**, *473*, 51–87.

[21] R. Saito, A. Jorio, A. G. Souza Filho, G. Dresselhaus, M. S. Dresselhaus, M. A. Pimenta, *Phys. Rev. Lett.* **2001**, *88*, 027401.

[22] A. K. Gupta, T. J. Russin, H. R. Gutierrez, P. C. Eklund, *ACS Nano* **2009**, *3*, 45–52.

[23] A. C. Ferrari, *Solid State Commun.* **2007**, *143*, 47–57.

[24] A. C. Ferrari, J. C. Meyer, V. Scardaci, C. Casiraghi, M. Lazzeri, F. Mauri, S. Piscanec, D. Jiang, K. S. Novoselov, S. Roth, A. K. Geim, *Phys. Rev. Lett.* **2006**, *97*, 187401.

[25] L. M. Malard, J. Nilsson, D. C. Elias, J. C. Brant, F. Plentz, E. S. Alves, A. H. Castro Neto, M. A. Pimenta, *Phys. Rev. B* **2007**, *76*, 201401.

[26] Y. Y. Wang, Z. H. Ni, Z. X. Shen, H. M. Wang, Y. H. Wu, *Appl. Phys. Lett.* **2008**, *92*, 043121.

[27] Y. K. Koh, M.-H. Bae, D. G. Cahill, E. Pop, *ACS Nano* **2010**, *5*, 269–274.

[28] P. H. Tan, W. P. Han, W. J. Zhao, Z. H. Wu, K. Chang, H. Wang, Y. F. Wang, N. Bonini, N. Marzari, N. Pugno, G. Savini, A. Lombardo, A. C. Ferrari, *Nat. Mater.* **2012**, *11*, 294–300.

[29] C. H. Lui, L. M. Malard, S. Kim, G. Lantz, F. E. Laverge, R. Saito, T. F. Heinz, *Nano Lett.* **2012**, *12*, 5539–5544.

[30] L. G. Cançado, M. A. Pimenta, B. R. A. Neves, M. S. S. Dantas, A. Jorio, *Phys. Rev. Lett.* **2004**, *93*, 247401.

[31] Y. You, Z. Ni, T. Yu, Z. Shen, *Appl. Phys. Lett.* **2008**, *93*, 163112.

[32] C. Casiraghi, A. Hartschuh, H. Qian, S. Piscanec, C. Georgi, A. Fasoli, K. S. Novoselov, D. M. Basko, A. C. Ferrari, *Nano Lett.* **2009**, *9*, 1433–1441.

[33] B. Krauss, P. Nemes-Incze, V. Skakalova, L. P. Biro, K. von Klitzing, J. H. Smet, *Nano Lett.* **2010**, *10*, 4544–4548.

[34] H. T. Liu, S. M. Ryu, Z. Y. Chen, M. L. Steigerwald, C. Nuckolls, L. E. Brus, *J. Am. Chem. Soc.* **2009**, *131*, 17099–17101.

[35] E. H. Hwang, S. Adam, S. Das Sarma, *Phys. Rev. Lett.* **2007**, *98*, 186806.

[36] J. H. Chen, C. Jang, S. Adam, M. S. Fuhrer, E. D. Williams, M. Ishigami, *Nat. Phys.* **2008**, *4*, 377–381.

[37] Z. H. Ni, W. Chen, X. F. Fan, J. L. Kuo, T. Yu, A. T. S. Wee, Z. X. Shen, *Phys. Rev. B* **2008**, *77*, 115416.

[38] Y. Y. Wang, Z. H. Ni, T. Yu, Z. X. Shen, H. M. Wang, Y. H. Wu, W. Chen, A. T. S. Wee, *J. Phys. Chem. C* **2008**, *112*, 10637–10640.

[39] C. Casiraghi, S. Pisana, K. S. Novoselov, A. K. Geim, A. C. Ferrari, *Appl. Phys. Lett.* **2007**, *91*, 233108.

[40] J. Yan, Y. Zhang, P. Kim, A. Pinczuk, *Phys. Rev. Lett.* **2007**, *98*, 166802.

[41] Z. H. Ni, T. Yu, Z. Q. Luo, Y. Y. Wang, L. Liu, C. P. Wong, J. Miao, W. Huang, Z. X. Shen, *ACS Nano* **2009**, *3*, 569–574.

[42] A. Das, S. Pisana, B. Chakraborty, S. Piscanec, S. K. Saha, U. V. Waghmare, K. S. Novoselov, H. R. Krishnamurthy, A. K. Geim, A. C. Ferrari, A. K. Sood, *Nat. Nanotechnol.* **2008**, *3*, 210–215.

[43] S. Pisana, M. Lazzeri, C. Casiraghi, K. S. Novoselov, A. K. Geim, A. C. Ferrari, F. Mauri, *Nat. Mater.* **2007**, *6*, 198–201.

[44] S. Roddaro, P. Pingue, V. Piazza, V. Pellegrini, F. Beltram, *Nano Lett.* **2007**, *7*, 2707–2710.

[45] I. Jung, M. Pelton, R. Piner, D. A. Dikin, S. Stankovich, S. Watcharotone, M. Hausner, R. S. Ruoff, *Nano Lett.* **2007**, *7*, 3569–3575.

[46] P. Blake, E. W. Hill, A. H. C. Neto, K. S. Novoselov, D. Jiang, R. Yang, T. J. Booth, A. K. Geim, *Appl. Phys. Lett.* **2007**, *91*, 063124.

[47] D. S. L. Abergel, A. Russell, V. I. Fal'ko, *Appl. Phys. Lett.* **2007**, *91*, 063125.

[48] D. Yoon, H. Moon, Y.-W. Son, J. S. Choi, B. H. Park, Y. H. Cha, Y. D. Kim, H. Cheong, *Phys. Rev. B* **2009**, *80*, 125422.

[49] W. Ren, R. Saito, L. Gao, F. Zheng, Z. Wu, B. Liu, M. Furukawa, J. Zhao, Z. Chen, H.-M. Cheng, *Phys. Rev. B* **2010**, *81*, 035412.

[50] L. Gao, W. Ren, B. Liu, R. Saito, Z.-S. Wu, S. Li, C. Jiang, F. Li, H.-M. Cheng, *ACS Nano* **2009**, *3*, 933–939.

[51] K. F. Domke, B. Pettinger, *J. Raman Spectrosc.* **2009**, *40*, 1427–1433.

[52] Y. Saito, P. Verma, K. Masui, Y. Inouye, S. Kawata, *J. Raman Spectrosc.* **2009**, *40*, 1434–1440.

[53] J. Lee, S. Shim, B. Kim, H. S. Shin, *Chem. Eur. J.* **2011**, *17*, 2381–2387.

[54] F. Schedin, E. Lidorikis, A. Lombardo, V. G. Kravets, A. K. Geim, A. N. Grigorenko, K. S. Novoselov, A. C. Ferrari, *ACS Nano* **2010**, *4*, 5617–5626.

[55] L. D'Urso, G. Forte, P. Russo, C. Caccamo, G. Compagnini, O. Puglisi, *Carbon* **2011**, *49*, 3149–3157.

[56] Y. Ouyang, L. Chen, *J. Mol. Struct.* **2011**, *992*, 48–51.

[57] M. Ghislandi, G. G. Hoffmann, E. Tkalya, L. Xue, G. De With, *Appl. Spectrosc. Rev.* **2012**, *47*, 371–381.

[58] J. Huang, C. Zong, H. Shen, M. Liu, B. Chen, B. Ren, Z. Zhang, *Small* **2012**, *8*, 2577–2584.

[59] J. Niu, V. G. Truong, H. Huang, S. Tripathy, C. Y. Qiu, A. T. S. Wee, T. Yu, H. Yang, *Appl. Phys. Lett.* **2012**, *100*, 191601.

[60] P. Wang, D. Zhang, L. Li, Z. Li, L. Zhang, Y. Fang, *Plasmonics* **2012**, *7*, 555–561.

[61] A. Urich, A. Pospischil, M. M. Furchi, D. Dietze, K. Unterrainer, T. Mueller, *Appl. Phys. Lett.* **2012**, *101*, 153113.

[62] V. G. Kravets, F. Schedin, R. Jalil, L. Britnell, K. S. Novoselov, A. N. Grigorenko, *J. Phys. Chem. C* **2012**, *116*, 3882–3887.

[63] J. Lee, K. S. Novoselov, H. S. Shin, *ACS Nano* **2011**, *5*, 608–612.

[64] W. G. Xu, X. Ling, J. Q. Xiao, M. S. Dresselhaus, J. Kong, H. X. Xu, Z. F. Liu, J. Zhang, *Proc. Natl. Acad. Sci. USA* **2012**, *109*, 9281–9286.

[65] W. G. Xu, J. Q. Xiao, Y. F. Chen, Y. B. Chen, X. Ling, J. Zhang, *Adv. Mater.* **2013**, *25*, 928–933.

[66] Z. Liu, J. T. Robinson, X. M. Sun, H. J. Dai, *J. Am. Chem. Soc.* **2008**, *130*, 10876–10877.

[67] M. Pumera, *Mater. Today* **2011**, *14*, 308–315.

[68] J. H. Shen, Y. H. Zhu, X. L. Yang, C. Z. Li, *Chem. Commun.* **2012**, *48*, 3686–3699.

[69] Z.-Q. Tian, B. Ren, D.-Y. Wu, *J. Phys. Chem. B* **2002**, *106*, 9463–9483.

[70] B. Ren, G.-K. Liu, X.-B. Lian, Z.-L. Yang, Z.-Q. Tian, *Anal. Bioanal. Chem.* **2007**, *388*, 29–45.

[71] X. T. Wang, W. S. Shi, G. W. She, L. X. Mu, *Phys. Chem. Chem. Phys.* **2012**, *14*, 5891–5901.

[72] L. M. Xie, X. Ling, Y. Fang, J. Zhang, Z. F. Liu, *J. Am. Chem. Soc.* **2009**, *131*, 9890–9891.

[73] J. M. Benevides, S. A. Overman, G. J. Thomas, *J. Raman Spectrosc.* **2005**, *36*, 279–299.

[74] D. V. Martyshkin, R. C. Ahuja, A. Kudriavtsev, S. B. Mirov, *Rev. Sci. Instrum.* **2004**, *75*, 630–635.

[75] R. F. Begley, A. B. Harvey, R. L. Byer, *Appl. Phys. Lett.* **1974**, *25*, 387–390.

[76] D. W. McCamant, P. Kukura, S. Yoon, R. A. Mathies, *Rev. Sci. Instrum.* **2004**, *75*, 4971–4980.

[77] R. S. Swathi, K. L. Sebastian, *J. Chem. Phys.* **2008**, *129*, 054703.

[78] X. Ling, L. Xie, Y. Fang, H. Xu, H. Zhang, J. Kong, M. S. Dresselhaus, J. Zhang, Z. Liu, *Nano Lett.* **2010**, *10*, 553–561.

[79] X. Ling, Graphene Enhanced Raman Scattering Effect **2012**, PhD thesis, Beijing, Peking University, China.

[80] X. Ling, J. Zhang, *J. Phys. Chem. C* **2011**, *115*, 2835–2840.

[81] S. Huh, J. Park, Y. S. Kim, K. S. Kim, B. H. Hong, J.-M. Nam, *ACS Nano* **2011**, *5*, 9799–9806.

[82] X. X. Yu, H. B. Cai, W. H. Zhang, X. J. Li, N. Pan, Y. Luo, X. P. Wang, J. G. Hou, *ACS Nano* **2011**, *5*, 952–958.

[83] H. Cheng, Y. Zhao, Y. Fan, X. Xie, L. Qu, G. Shi, *ACS Nano* **2012**, *6*, 2237–2244.

[84] Y. Y. Wang, Z. H. Ni, L. Aizhi, Z. Zafar, Y. Zhang, Z. H. Ni, S. L. Qu, T. Qiu, T. Yu, Z. X. Shen, *Appl. Phys. Lett.* **2011**, *99*, 233103.

[85] J. Liu, H. Cai, X. Yu, K. Zhang, X. Li, J. Li, N. Pan, Q. Shi, Y. Luo, X. Wang, *J. Phys. Chem. C* **2012**, *116*, 15741–15746.

[86] M. Begliarbekov, O. Sul, J. Santanello, N. Ai, X. Zhang, E. H. Yang, S. Strauf, *Nano Lett.* **2011**, *11*, 1254–1258.

[87] M. Moskovits, *Rev. Mod. Phys.* **1985**, *57*, 783–826.

[88] A. Campion, P. Kambhampati, *Chem. Soc. Rev.* **1998**, *27*, 241–250.

[89] A. Otto, *J. Raman Spectrosc.* **2005**, *36*, 497–509.

[90] G. C. Schatz, M. A. Young, R. P. Van Duyne, *Top. Appl. Phys.* **2006**, *103*, 19–45.

[91] J. A. Scholl, A. L. Koh, J. A. Dionne, *Nature* **2012**, *483*, 421–427.

[92] A. N. Grigorenko, M. Polini, K. S. Novoselov, *Nat. Photonics* **2012**, *6*, 749–758.

[93] A. Otto, *Phys. Status Solidi A* **2001**, *188*, 1455–1470.

[94] X. Ling, J. Zhang, *Small* **2010**, *6*, 2020–2025.

[95] M. Osawa, N. Matsuda, K. Yoshii, I. Uchida, *J. Phys. Chem.* **1994**, *98*, 12702–12707.

[96] T. Shegai, A. Vaskevich, I. Rubinstein, G. Haran, *J. Am. Chem. Soc.* **2009**, *131*, 14390–14398.

[97] H. Xu, L. M. Xie, H. L. Zhang, J. Zhang, *ACS Nano* **2011**, *5*, 5338–5344.

[98] H. Xu, Y. B. Chen, W. G. Xu, H. L. Zhang, J. Kong, M. S. Dresselhaus, J. Zhang, *Small* **2011**, *7*, 2945–2952.

[99] H. Xu, Y. B. Chen, J. Zhang, H. L. Zhang, *Small* **2012**, *8*, 2833–2840.

[100] X. Ling, L. G. Moura, M. A. Pimenta, J. Zhang, *J. Phys. Chem. C* **2012**, *116*, 25112–25118.

[101] E. S. Thrall, A. C. Crowther, Z. H. Yu, L. E. Brus, *Nano Lett.* **2012**, *12*, 1571–1577.

[102] X. Ling, J. X. Wu, W. G. Xu, J. Zhang, *Small* **2012**, *8*, 1365–1372.

[103] X. Ling, J. Zhang, *Acta Phys.—Chim. Sin.* **2012**, *28*, 2355–2362.

[104] C. Xu, X. Wang, *Small* **2009**, *5*, 2212–2217.

[105] K. Jasuja, V. Berry, *ACS Nano* **2009**, *3*, 2358–2366.

[106] X. Fu, F. Bei, X. Wang, S. O'Brien, J. R. Lombardi, *Nanoscale* **2010**, *2*, 1461–1466.

[107] J. Huang, L. M. Zhang, B. A. Chen, N. Ji, F. H. Chen, Y. Zhang, Z. J. Zhang, *Nanoscale* **2010**, *2*, 2733–2738.

[108] Y. Y. Wang, Z. H. Ni, H. L. Hu, Y. F. Hao, C. P. Wong, T. Yu, J. T. L. Thong, Z. X. Shen, *Appl. Phys. Lett.* **2010**, *97*, 163111.

[109] L. Chih-Yi, L. Keng-Chih, C. Waileong, T. Chia-hao, L. Chuan-Pu, T. Yonhua, *Opt. Express* **2011**, *19*, 17092–17098.

[110] C. Jianli, Z. Xianliang, W. Huan, Z. Weitao, *Thin Solid Films* **2011**, *520*, 179–185.

[111] X. Liu, L. Cao, W. Song, K. Ai, L. Lu, *ACS Appl. Mater. Inter.* **2011**, *3*, 2944–2952.

[112] G. Lu, H. Li, C. Liusman, Z. Yin, S. Wu, H. Zhang, *Chem. Sci.* **2011**, *2*, 1817–1821.

[113] W. Ren, Y. X. Fang, E. K. Wang, *ACS Nano* **2011**, *5*, 6425–6433.

[114] P. Shugang, L. Xiaoheng, W. Xin, *Mater. Charact.* **2011**, *62*, 1094–1101.

[115] S. Sun, P. Wu, *Phys. Chem. Chem. Phys.* **2011**, *13*, 21116–21120.

[116] Y. K. Yang, C. E. He, W. J. He, L. J. Yu, R. G. Peng, X. L. Xie, X. B. Wang, Y. W. Mai, *J. Nanopart. Res.* **2011**, *13*, 5571–5581.

[117] Z. Zhang, F. Xu, W. Yang, M. Guo, X. Wang, B. Zhanga, J. Tang, *Chem. Commun.* **2011**, *47*, 6440–6442.

[118] S. He, K.-K. Liu, S. Su, J. Yan, X. Mao, D. Wang, Y. He, L.-J. Li, S. Song, C. Fan, *Anal. Chem.* **2012**, *84*, 4622–4627.

[119] Y. Hu, L. Lu, J. Liu, W. Chen, *J. Mater. Chem.* **2012**, *22*, 11994–12000.

[120] X. K. Kong, Q. W. Chen, *J. Mater. Chem.* **2012**, *22*, 15336–15341.

[121] X. Li, B. K. Tay, J. Li, D. Tan, C. W. Tan, K. Liang, *Nanoscale Res. Lett.* **2012**, *7*, 205.

[122] F. Lu, S. H. Zhang, H. J. Gao, H. Jia, L. Q. Zheng, *ACS Appl. Mater. Inter.* **2012**, *4*, 3278–3284.

[123] A. N. Sidorov, G. W. Slawinski, A. H. Jayatissa, F. P. Zamborini, G. U. Sumanasekera, *Carbon* **2012**, *50*, 699–705.

[124] K. Zhang, *Appl. Surf. Sci.* **2012**, *258*, 7327–7329.

[125] Y. W. Zhang, S. Liu, L. Wang, X. Y. Qin, J. Q. Tian, W. B. Lu, G. H. Chang, X. P. Sun, *RSC Adv.* **2012**, *2*, 538–545.

[126] H. Zhao, H. Fu, T. Zhao, L. Wang, T. Tan, *J. Colloid Interface Sci.* **2012**, *375*, 30–34.

[127] X. Y. Zhang, J. Zhao, A. V. Whitney, J. W. Elam, R. P. Van Duyne, *J. Am. Chem. Soc.* **2006**, *128*, 10304–10309.

[128] H. X. Xu, *Appl. Phys. Lett.* **2004**, *85*, 5980–5982.

[129] F. X. Liu, Z. S. Cao, C. J. Tang, L. Chen, Z. L. Wang, *ACS Nano* **2010**, *4*, 2643–2648.

[130] Q. Z. Hao, B. Wang, J. A. Bossard, B. Kiraly, Y. Zeng, I. K. Chiang, L. Jensen, D. H. Werner, T. J. Huang, *J. Phys. Chem. C* **2012**, *116*, 7249–7254.

[131] V. Georgakilas, M. Otyepka, A. B. Bourlinos, V. Chandra, N. Kim, K. C. Kemp, P. Hobza, R. Zboril, K. S. Kim, *Chem. Rev.* **2012**, *112*, 6156–6214.

[132] J. E. Rowe, C. V. Shank, D. A. Zwemer, C. A. Murray, *Phys. Rev. Lett.* **1980**, *44*, 1770–1773.

[133] I. Pockrand, A. Otto, *Solid State Commun.* **1980**, *35*, 861–865.

[134] M. S. Anderson, *Appl. Phys. Lett.* **2000**, *76*, 3130–3132.

[135] B. Pettinger, G. Picardi, R. Schuster, G. Ertl, *Single Mol.* **2002**, *3*, 285–294.

[136] R. G. Freeman, K. C. Grabar, K. J. Allison, R. M. Bright, J. A. Davis, A. P. Guthrie, M. B. Hommer, M. A. Jackson, P. C. Smith, D. G. Walter, M. J. Natan, *Science* **1995**, *267*, 1629–1632.

[137] C. A. Mirkin, L. D. Qin, S. L. Zou, C. Xue, A. Atkinson, G. C. Schatz, *Proc. Natl. Acad. Sci. USA* **2006**, *103*, 13300–13303.

[138] H. Im, K. C. Bantz, N. C. Lindquist, C. L. Haynes, S.-H. Oh, *Nano Lett.* **2010**, *10*, 2231–2236.

[139] D.-K. Lim, K.-S. Jeon, J.-H. Hwang, H. Kim, S. Kwon, Y. D. Suh, J.-M. Nam, *Nat. Nanotechnol.* **2011**, *6*, 452–460.

[140] P. T. Anastas, *Crit. Rev. Anal. Chem.* **1999**, *29*, 167–175.

[141] L. H. Keith, L. U. Gron, J. L. Young, *Chem. Rev.* **2007**, *107*, 2695–2708.

[142] S. Armenta, S. Garrigues, M. Delaguardia, *TrAC, Trends Anal. Chem.* **2008**, *27*, 497–511.

[143] M. Tobiszewski, A. Mechlińska, J. Namieśnik, *Chem. Soc. Rev.* **2010**, *39*, 2869–2878.

[144] F. Schwierz, *Nat. Nanotechnol.* **2010**, *5*, 487–496.